

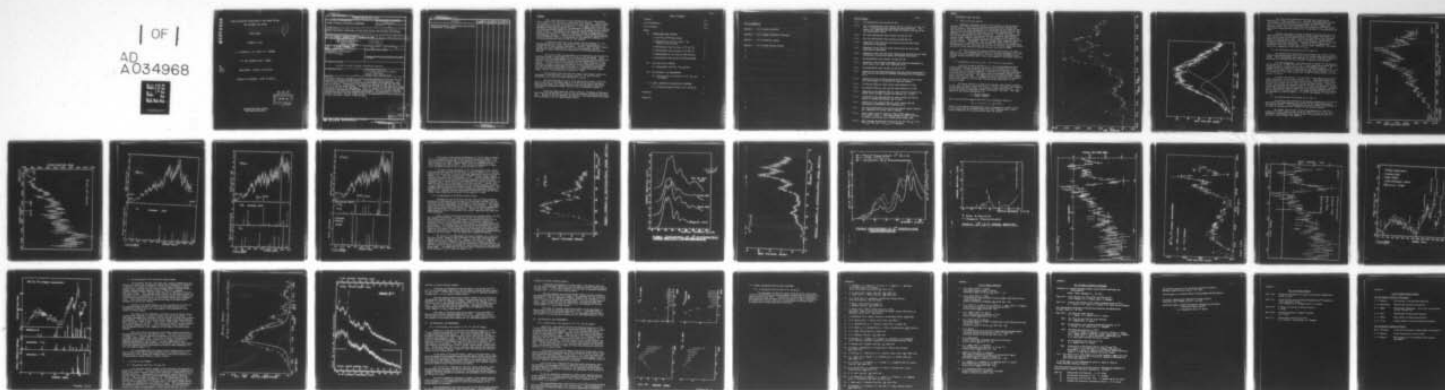
AD-A034 968

MELBOURNE UNIV PARKVILLE (AUSTRALIA) SCHOOL OF PHYSICS F/6 20/8  
ATOMIC AND NUCLEAR INTERACTIONS OF HIGH ENERGY PHOTONS AND ELEC--ETC(U)  
SEP 75 E G MUIRHEAD, B M SPICER, M N THOMPSON DA-ARO-D-31-124-73-672

NL

UNCLASSIFIED

| OF |  
AD  
A034968



END

DATE  
FILMED  
3-77

ADA 034968

ATOMIC AND NUCLEAR INTERACTIONS OF HIGH ENERGY PHOTONS  
AND ELECTRONS WITH MATTER

FINAL REPORT

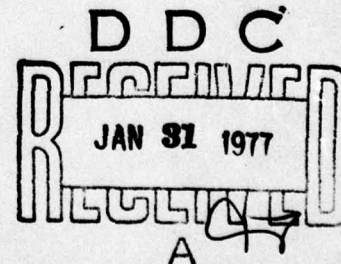
OCTOBER 15, 1975

E. G. MUIRHEAD, B. M. SPICER, M. N. THOMPSON

U.S. ARMY RESEARCH OFFICE - DURHAM

GRANT NUMBER - DA-ARO-D-31-124-73-G72

UNIVERSITY OF MELBOURNE - SCHOOL OF PHYSICS



APPROVED FOR PUBLIC RELEASE;  
DISTRIBUTION UNLIMITED.

Good  
FC.

Unclassified

## Security Classification

## DOCUMENT CONTROL DATA - R &amp; D

(Security classification of title, body of abstract and indexing annotation must be entered when the overall report is classified)

1. ORIGINATING ACTIVITY (Corporate author)		2a. REPORT SECURITY CLASSIFICATION	
School of Physics, University of Melbourne		Unclassified	
3. REPORT TITLE		2b. GROUP	
Atomic and Nuclear Interactions of High Energy Photons and Electrons with Matter.		NA	
4. DESCRIPTIVE NOTES (Type of report and inclusive dates)			
9/ Final Report - January 1, 1973 - December 31, 1974 1 Jan 73-31 Dec 74			
5. AUTHOR(S) (First name, middle initial, last name)			
10 Edmund G. Muirhead, Brian M. Spicer Maxwell N. Thompson			
6. REPORT DATE		7a. TOTAL NO. OF PAGES	7b. NO. OF REFS
15 11 29 September, 1975		40	22
8. CONTRACT OR GRANT NO.		9a. ORIGINATOR'S REPORT NUMBER(S)	
DA-ARO-D-31-124-73-672 New			
9. PROJECT NO.		9b. OTHER REPORT NO(S) (Any other numbers that may be assigned this report)	
P-F-54-P			
10. DISTRIBUTION STATEMENT			
Approved for public release; distribution unlimited.			
11. SUPPLEMENTARY NOTES		12. SPONSORING MILITARY ACTIVITY	
		U. S. Army Research Office-Durham Box CM, Duke Station Durham, North Carolina 27706	
13. ABSTRACT			
<p>This report describes researches on nuclear photodisintegration carried out with the University of Melbourne 35 MeV betatron. It is divided into four sections. The first of these reports on <math>(\gamma, n)</math> cross section measurements which comprise the major part of the work. Photoneutron cross sections are reported for <math>^{16}\text{O}</math>, <math>^9\text{Be}</math>, <math>^{10}\text{B}</math>, <math>^{11}\text{B}</math>, <math>^{12}\text{C}</math>, <math>^{13}\text{C}</math>, <math>^{45}\text{Sc}</math> and natural osmium. The motivation for each of these studies is given, as are the results of the measurements. Parts II through IV are briefer, and describe respectively measurements of photoproton energy spectra from the zirconium isotopes, measurements and calculations regarding de-excitation <math>\gamma</math>-ray measurements in <math>^{19}\text{F}</math>, <math>^{31}\text{P}</math> and <math>^{39}\text{K}</math>, and finally the last stages of work on the determination of cross sections for K-shell ionization in nickel, silver and gold.</p> <p>gamma</p> <p>gamma</p>			

DD FORM 1473

REPLACES DD FORM 1473, 1 JAN 60, WHICH IS OBSOLETE FOR ARMY USE.

Unclassified

Security Classification

406 033	APY
---------	-----



**Security Classification**

14.

### KEY WORDS

**LINK A**

LINK 8

**LINK C**

**ROLE**

WT

**SOLE**

WT

**SOLE**

W

Photodisintegration; photoneutron cross section; photoprotons; K-ionization.

Unclassified

**Security Classification**



FOREWORD

This report describes projects undertaken with U.S. Army Research Office support at the University of Melbourne 35 MeV betatron. These projects are primarily in the field of photonuclear reactions, and use features of the betatron accelerator which are unique to it. For example, most of the work described in this report involves the measurement of photoneutron cross sections, and these measurements depend critically on the precise energy control inherent in the betatron. Unfortunately this advantage of precise energy control is offset by the necessity of using the continuous spectrum of bremsstrahlung as the bombarding radiation. Because of this offset, a previous report described a very substantial study of the limitations to the precision attainable in measuring photoneutron cross sections by this method<sup>1</sup>).

It should be noted that at the present time the betatron is a very low-powered source of x-rays, and because of this has been dropped as a research tool by many overseas laboratories. However, there is ample intensity available for work on photoneutron cross section measurement, and this constitutes a major reason for the concentration on that particular area of research.

The initial stages of measurements of the photoproton spectra from the zirconium isotopes of mass number 90, 91 and 92 are also described. These again utilised the bremsstrahlung from the 35 MeV betatron, and the protons were detected in cooled lithium-drifted silicon detectors manufactured in the laboratory. This work led to an investigation of the charge collection in such detectors, a report of which was published in Nuclear Instruments and Methods. The final photoproton measurements were made in a collaborative experiment carried out at the electron linear accelerator of Tohoku University, Sendai, Japan, with the kind cooperation of Professor K. Shoda.

The stretched x-ray beam (200  $\mu$ sec long) of the betatron enabled the measurement of de-excitation  $\gamma$ -ray spectra from  $^{19}\text{F}$ ,  $^{31}\text{P}$  and  $^{39}\text{K}$ , and a discussion of the result of these measurements is given.

The final theoretical work on the K-ionization of nickel, silver and gold by electrons in the energy range 2 to 20 MeV was carried out during the period of this grant, and a paper describing the work was read at the Fourth International Conference on Atomic Physics, held at Heidelberg, Germany in July 1974.

During the grant period the School of Physics, University of Melbourne, moved from its old building to a new one, and the betatron installation was moved also. Because of this circumstance, an extension of the grant period was sought, and was granted by the U.S. Army Research Office.

## TABLE OF CONTENTS

Foreword	(i)
List of Appendices	(iii)
List of Figures	(iv)
Report	
§ I PHOTONEUTRON CROSS SECTIONS	
I.1 The $^{16}\text{O}(\gamma, n)^{15}\text{O}$ Cross Section	1
I.2 Deformation in the $1f_{7/2}$ Shell - The $^{45}\text{Sc}(\gamma, n)$ Cross Section	1
I.3 Photoneutron Cross Sections of $^{10}\text{B}$ and $^{11}\text{B}$	2
I.4 Photoneutron Cross Sections of $^{12}\text{C}$ and $^{13}\text{C}$	2
I.5 Remeasurement of the $^9\text{Be}(\gamma, n)$ Cross Section	3
I.6 Photoneutron Cross Section of Natural Osmium	4
§ II $(\gamma, p)$ AND $(e, e'p)$ STUDIES	
II.1 Photoprotons from $^{90}\text{Zr}$ , $^{91}\text{Zr}$ and $^{92}\text{Zr}$	4
§ III DE-EXCITATION $\gamma$ -RAY MEASUREMENTS	
III.1 De-excitation $\gamma$ -ray Spectra in $^{19}\text{F}$ , $^{31}\text{P}$ , and $^{39}\text{K}$ Targets	5
IV K-SHELL IONIZATION BY RELATIVISTIC ELECTRONS	
IV.1 K-ionization Cross Sections in Ni, Ag and Au	6
References	7
Appendices	



List of Appendices

Appendix 1 List of papers published.

Appendix 2 List of papers presented at meetings.

Appendix 3 List of technical reports.

Appendix 4 List of Higher Degrees granted.



List of Figures

- I.1.1. The photoneutron cross section of  $^{16}\text{O}$ .
- I.2.1. The total photoneutron cross section,  $\sigma(\gamma, n) + \sigma(\gamma, pn) + \sigma(\gamma, 2n)$  for  $^{45}\text{Sc}$ . The horizontal bars indicate the resolution width. The smooth curve represents the Danos model fit which is the sum of the two dashed Lorentz curves.
- I.3.1. The total photoneutron cross section,  $\sigma(\gamma, Tn)$  for  $^{10}\text{B}$ .
- I.3.2. The total photoneutron cross section,  $\sigma(\gamma, Tn)$  for  $^{11}\text{B}$ .
- I.3.3. Comparison of the  $^{10}\text{B}(\gamma, Tn)$  cross section with the shell model calculation of Shackleton.
- I.3.4. Comparison of the  $^{11}\text{B}(\gamma, Tn)$  cross section with the shell model calculation of Shackleton.
- I.3.5. Comparison of the  $^{11}\text{B}(\gamma, Tn)$  cross section with the particle-hole model calculations of Spicer and Fraser, and Kurdyumov and Smirnov.
- I.4.1. The photoneutron cross section,  $\sigma(\gamma, Tn)$  for  $^{12}\text{C}$ .
- I.4.2. Comparison of the present measurement with previous measurements by Van de Vyver et al, Cook et al, and Fultz et al.
- I.4.3. The photoneutron cross section,  $\sigma(\gamma, Tn)$  for  $^{13}\text{C}$ .
- I.4.4. Comparison of the present measurement with the previous measurement by Cook, and with the inelastic electron scattering result of Bergstrom et al.
- I.4.5. Comparison of the low energy section of the  $^{13}\text{C}(\gamma, n)$  cross section with mono-energetic  $\gamma$ -ray results of Green and Donahue.
- I.5.1. The measured  $^9\text{Be}(\gamma, n)$  cross section from threshold to 8 MeV.
- I.5.2. The measured  $^9\text{Be}(\gamma, n)$  cross section from threshold to 27 MeV.
- I.5.3. Comparison of the measured  $^9\text{Be}(\gamma, n)$  cross section with earlier low energy results of Edge, Jakobson and Bertozzi ( $E_\gamma < 8$  MeV).
- I.5.4. Comparison of the measured  $^9\text{Be}(\gamma, n)$  cross section with earlier results of Nathans and Halpern, and of Costa.
- I.5.5. Comparison of the measured  $^9\text{Be}(\gamma, n)$  cross section with the calculations of Shackleton and of Majling et al.
- I.6.1. The total photoneutron cross section for natural osmium, together with comparison with theory (due to Greiner).
- II.1.1. Proton spectra from the reactions  $^{90}\text{Zr}(\gamma, p)^{89}\text{Y}$  (upper) and  $^{91}\text{Zr}(\gamma, p)^{90}\text{Y}$  (lower). The bremsstrahlung end-point was 30 MeV. The spectra are plotted with a common proton energy scale.
- III.1.1. Cross sections derived from yield curves for the  $^{19}\text{F}(\gamma, p_1 \gamma')^{18}\text{O}$ ,  $^{19}\text{F}(\gamma, p_2 \gamma')^{18}\text{O}$ , and  $^{19}\text{F}(\gamma, \alpha_{1,2} \gamma')^{15}\text{N}$  reactions.

## I. PHOTONEUTRON CROSS SECTIONS

I.1  $^{16}\text{O}(\gamma, n)^{15}\text{O}$  Cross Section

Immediately following the move of the betatron to the new Physics Building, the  $^{16}\text{O}(\gamma, n)^{15}\text{O}$  cross section was measured using a Halpern-type neutron detector, and bremsstrahlung from the betatron as the radiation source. This reaction was chosen essentially as a calibrating reaction, both for the energy scale of the betatron itself and also for the neutron detector. This reaction is very suitable for both calibrations. Firstly, the structure in the  $^{16}\text{O}$  photo-absorption cross section has been measured by many different methods in many different laboratories, and the energies of its features are now well known. These energies therefore provide energy calibration points up to about  $24\frac{1}{2}$  MeV. Furthermore, since for energies below 25 MeV the great majority of  $(\gamma, n)$  reactions leave the residual  $^{15}\text{O}$  nucleus in its ground state, the measurement of the yield curve for the  $^{16}\text{O}(\gamma, n)$  reaction exposes the neutron detector to a wide spectrum of neutron energies (from zero to 8 MeV).

The results of the yield curve measurement and analysis are shown in Figure I.1.1. The agreement in both energy of structure and shape of the cross section with previous measurements is very good, and gives confidence in the betatron energy calibration, and in the energy response of the neutron detection system.

I.2 Deformation in the  $1f_{7/2}$ -shell - the  $^{45}\text{Sc}(\gamma, n)$  cross section

Using the technique described in I.1 for the measurement of photo-neutron cross sections, the neutron production cross section for  $^{45}\text{Sc}$  was investigated. The motivation for this study was the observation<sup>2)</sup> by Malik and Scholz that a collective framework is required for a consistent description of the energy level structure and ground state electromagnetic moments of the early  $1f_{7/2}$ -shell nuclides. The suggestion that these nuclides form a deformed region of the periodic table is somewhat surprising, particularly for scandium whose atomic number is only one away from the closed proton shell of the calcium isotopes.

The target used was a 50 gram rod of natural, mono-isotopic scandium. In this case, the cross section sum,  $\{\sigma(\gamma, n) + \sigma(\gamma, np) + 2\sigma(\gamma, 2n)\}$ , was corrected for the double weighting of the  $(\gamma, 2n)$  process in the neutron detector. The statistical model, as described in Blatt & Weisskopf<sup>3)</sup>, was used. This model defines  $M$ , the neutron multiplicity, as

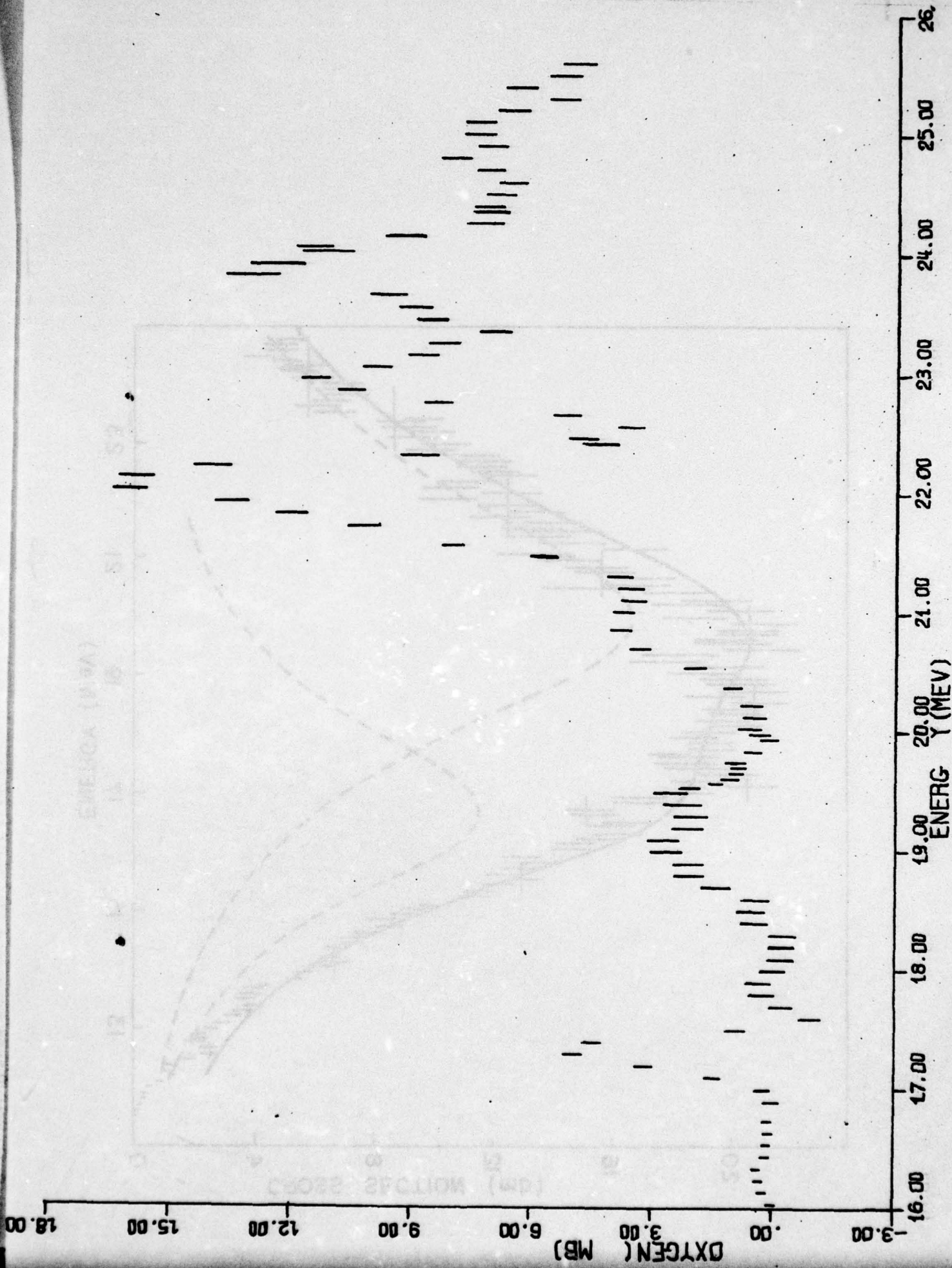
$$M = \frac{\sigma(\gamma, n) + 2\sigma(\gamma, 2n)}{\sigma(\gamma, n) + \sigma(\gamma, np)}$$

which, for excitation energies above the  $(\gamma, 2n)$  threshold, reduces to

$$M = 1 + (1-x) \left[ 1 - \left( 1 + \frac{\epsilon}{\theta} \right) e^{-\epsilon/\theta} \right],$$

where  $x$  is the fraction of photoneutron events proceeding by a direct process,  $\epsilon$  is the excess nuclear excitation above the  $(\gamma, 2n)$  threshold and  $\theta$  is the nuclear temperature of the target nucleus minus one nucleon.







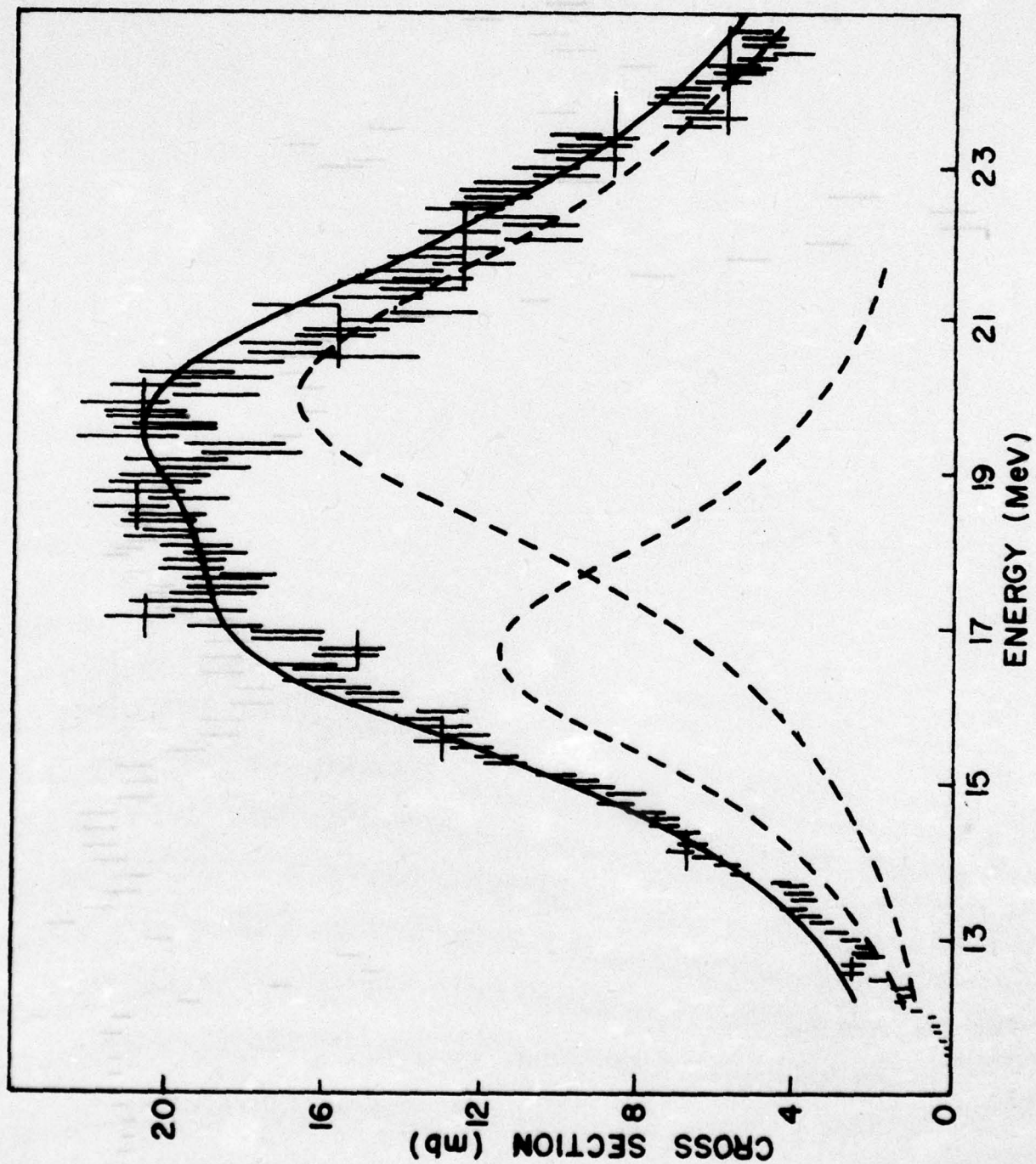


Figure T.2.1

The cross section obtained after making this correction for multiplicity is shown in Figure I.2.1. The most interesting aspect of this cross section is the large width at half-height, of approximately 8 MeV. Since it is known that a large deformation gives rise to a large giant resonance width<sup>4</sup>), the cross section was fitted using the sum of two Lorentz peaks whose integrated cross sections were in the ratio 1:2 as required by the model.

However, later work by Oikawa and Shoda<sup>5</sup>) indicates that the  $(\gamma, p)$  cross section for  $^{45}\text{Sc}$  (measuring protons of energy greater than 3 MeV) is of about the same shape as the neutron production cross section, but displaced upward in energy by about 4 MeV. This is attributed to a combination of isospin and deformation splitting of the giant resonance, and is, in our view an adequate qualitative explanation. The details of the quantitative separation of the cross section into  $T_+$  and  $T_-$  isospin components, and deformation split components are not nearly so clear.

### I.3 The Photoneutron Cross Sections of $^{10}\text{B}$ and $^{11}\text{B}$

The absolute total photoneutron cross sections for  $^{10}\text{B}$  and  $^{11}\text{B}$  were deduced from bremsstrahlung yield curves for the energy range from threshold to 28 MeV. These measurements were undertaken as part of a systematic series of measurements of photonuclear cross sections of nuclides in the 1p-shell.

For these measurements, the targets were 6.5 gm/cm<sup>2</sup> of  $^{10}\text{B}$  (99% pure) and 8.8 gm/cm<sup>2</sup> of  $^{11}\text{B}$  (80%  $^{11}\text{B}$ , 20%  $^{10}\text{B}$ ). These targets were pressed from the respective samples in powder form to obtain self-supporting pellets. No suitable model is available for correction for the double weighting of the  $(\gamma, 2n)$  reaction in nuclides as light as the boron isotopes, and so figures I.3.1 and I.3.2. show the  $(\gamma, T_n)$  cross sections for  $^{10}\text{B}$  and  $^{11}\text{B}$ , where  $\sigma(\gamma, T_n) = \sigma(\gamma, n) + \sigma(\gamma, pn) + 2\sigma(\gamma, 2n)$ .

For these two nuclides, it is possible to make comparison with theoretical calculations of the electric dipole states. Shackleton<sup>6</sup>) made shell model calculations of the non-natural parity states of all the 1p-shell nuclei, and this set of states does of course include the dipole states. Spicer and Fraser<sup>7</sup>) and Kurdyumov and Smirnov<sup>8</sup>) used the particle-hole formalism. Because of the approximations that had to be made in all these calculations, comparisons between the predicted dipole strengths and those obtained experimentally can only be expected to be qualitative. The comparison between these calculations and experiment is shown in figure I.3.3. for  $^{10}\text{B}$ , and figures I.3.4 and I.3.5. for  $^{11}\text{B}$ .

### I.4 The Photoneutron Cross Sections of $^{12}\text{C}$ and $^{13}\text{C}$

The absolute cross sections for photoneutron production in  $^{12}\text{C}$  and  $^{13}\text{C}$  were deduced from bremsstrahlung yield curves for the energy range between threshold and 29 MeV. These measurements constitute a further contribution to the study of photoneutron cross sections for the 1p-shell nuclides.

The targets used for this series of measurements were, for  $^{12}\text{C}$ , a cylinder of natural carbon of mass 269 gm and radius 2.2 cm; for the  $^{13}\text{C}$  measurement an amorphous carbon target of mass 13.5 gm enriched to 89.1%  $^{13}\text{C}$ , and with a 2.08% by weight iron impurity.



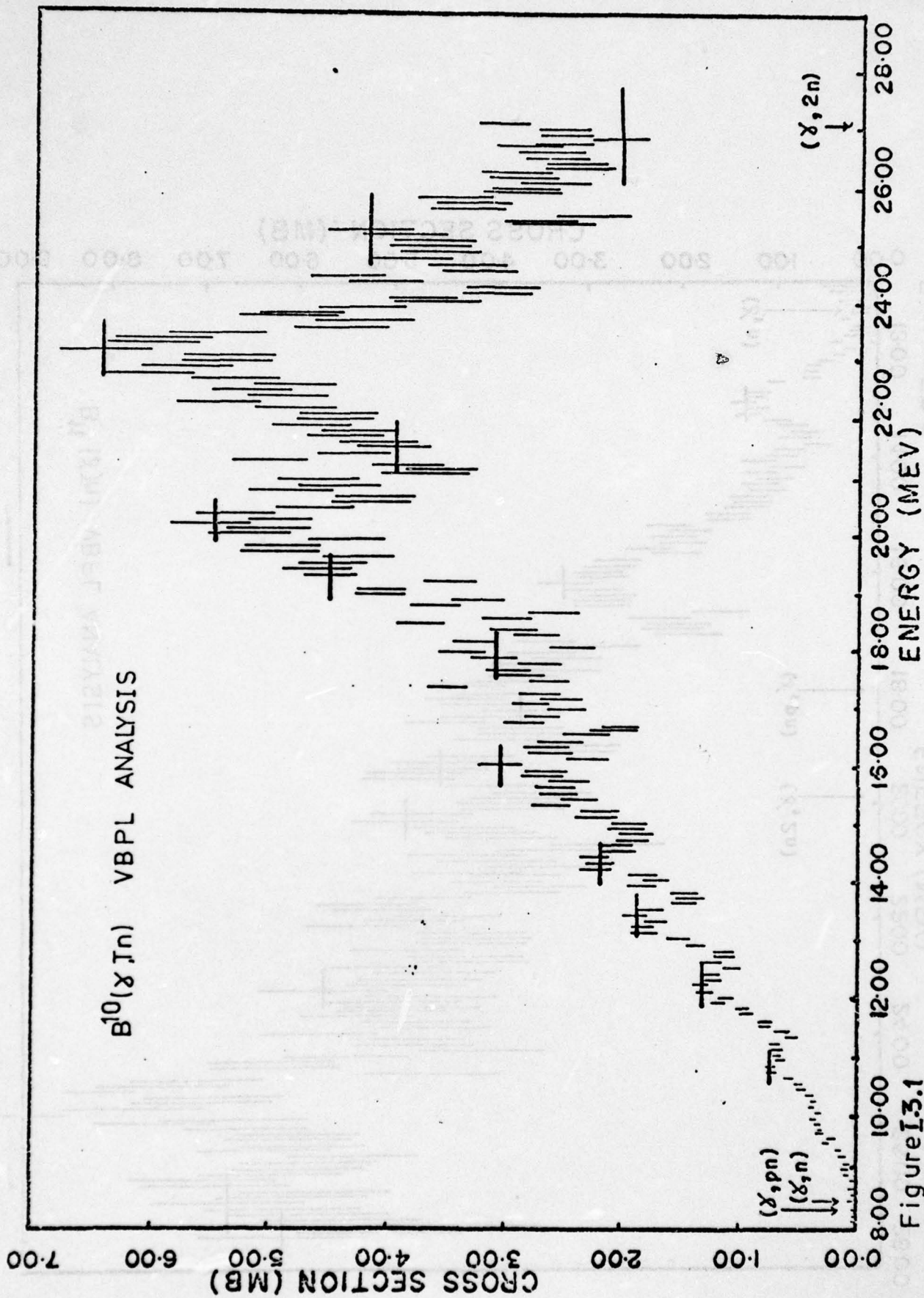


Figure I.3.1



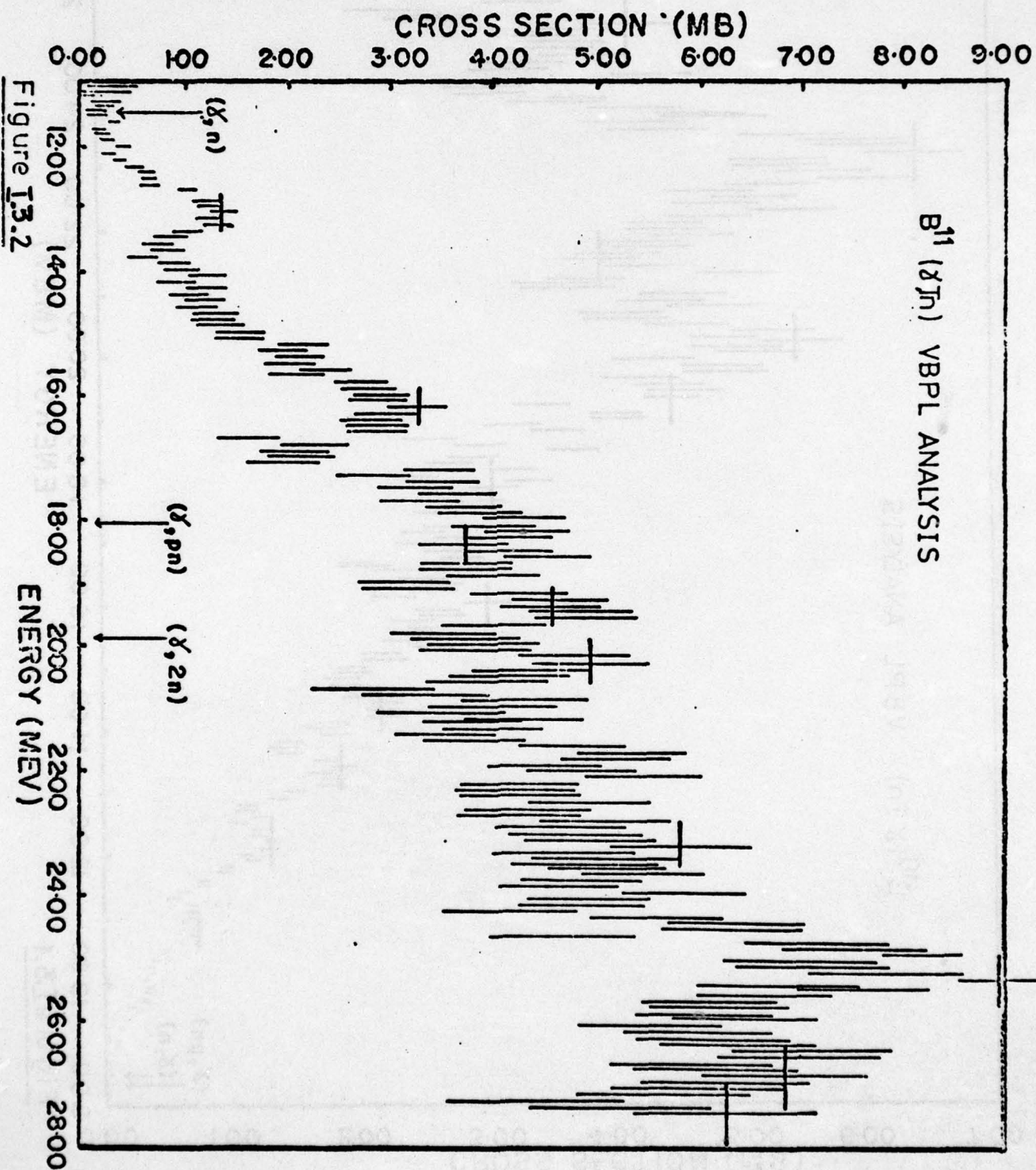


Figure 13.2

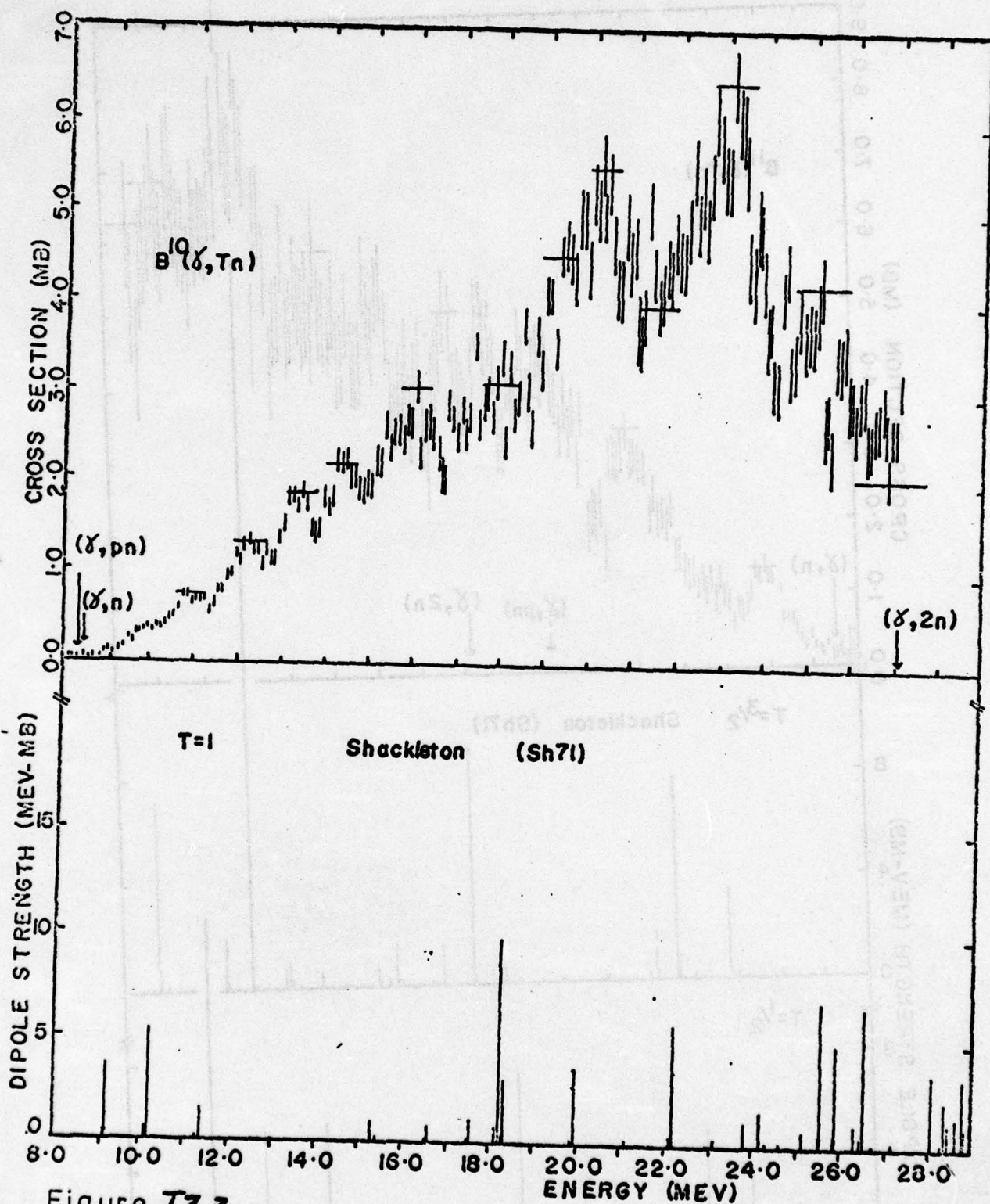


Figure I3.3



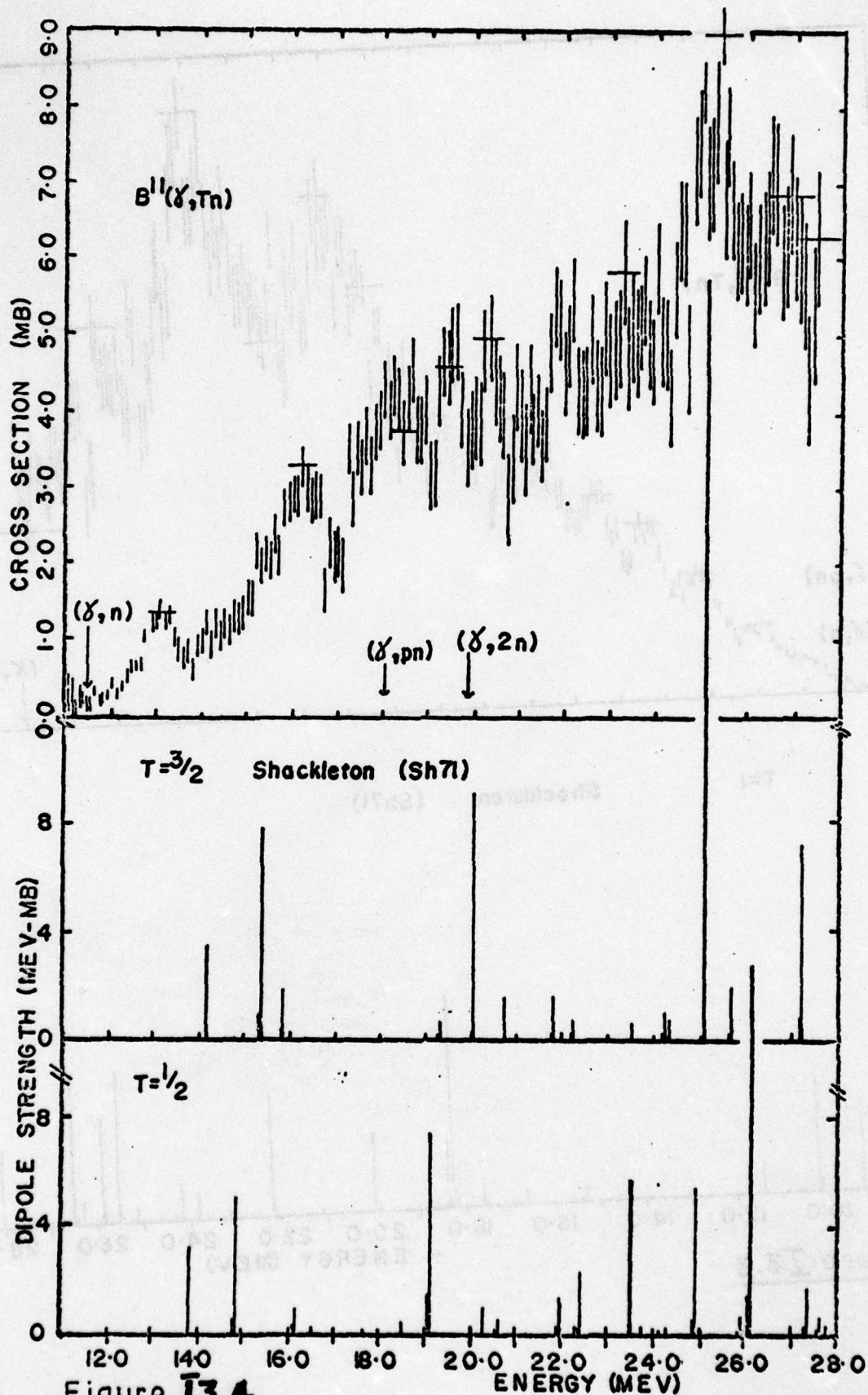


Figure 13.4



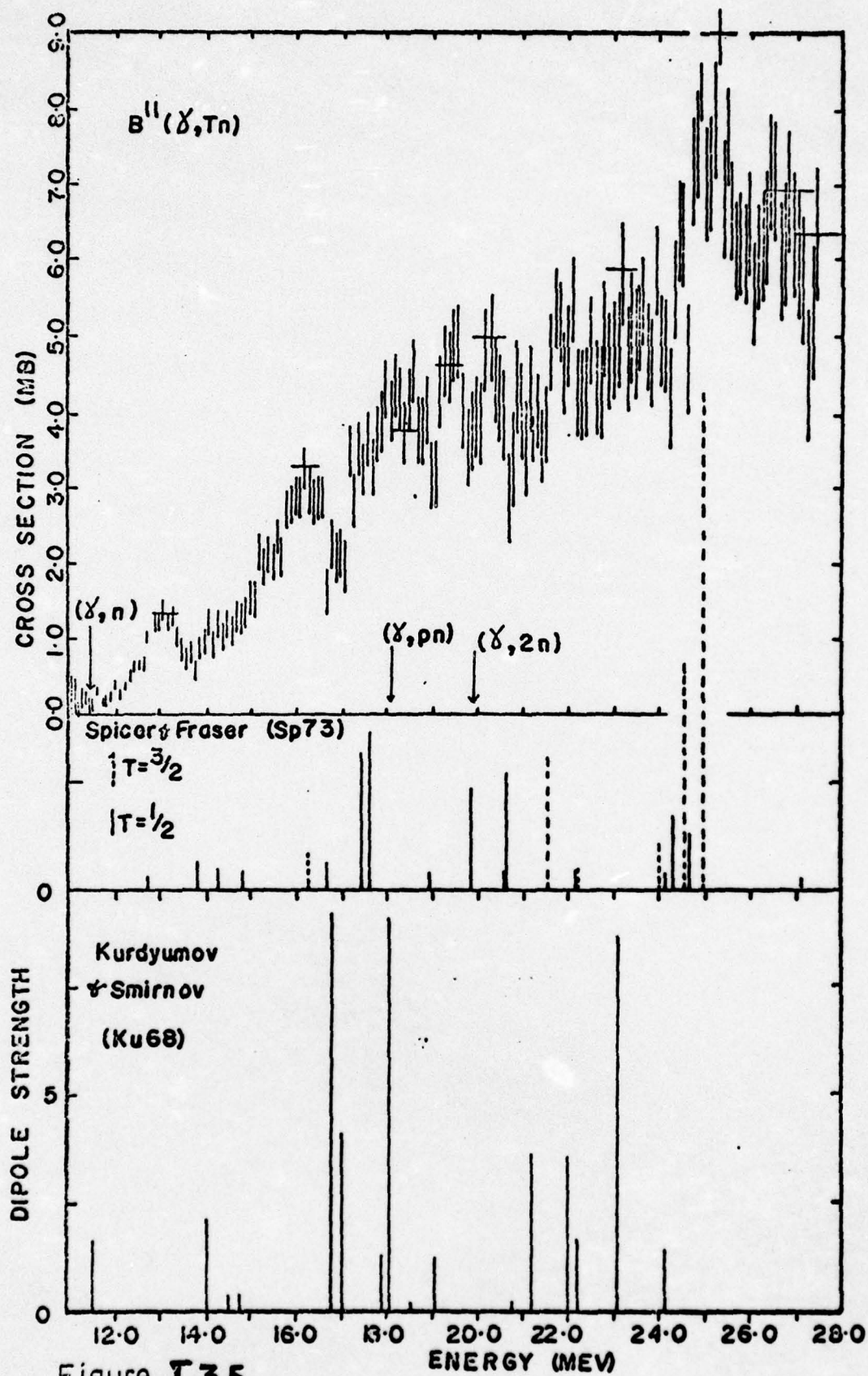


Figure **I.3.5.**

The results of the present measurements for  $^{12}\text{C}$  are shown in figure I.4.1., and comparison with the results of previous workers in figure I.4.2. The chief point of interest here is the appearance of a prominent dip in the cross section at 22.5 MeV, a feature which is more in agreement with the results presented by Cook et al<sup>16)</sup>. The other results presented in figure I.4.2. are those of Fultz et al<sup>17)</sup> and Van de Vyver et al<sup>18)</sup>.

The result of the measurement of the  $^{13}\text{C}$  photoneutron cross section, which was the main objective of this work, is shown in figure I.4.3., and comparison with the results of the only two other experimental results is given in figure I.4.4. These are an early result by Cook<sup>19)</sup>, and a recent inelastic electron scattering result of Bergstrom et al<sup>20)</sup>. The most notable feature of the present result is the resolution into two components of the main giant resonance peak, a feature which is just beginning to be evident in the electron scattering result, and is not present in the result of Cook. Further, the  $^{13}\text{C}(\gamma, n)$  cross section has been measured at nine separate energies, using monochromatic photons from neutron capture processes, by Green and Donahue<sup>21)</sup>. The agreement with the present work is fair, although the comparison, presented in figure I.4.5., indicates that the experimental resolution of the present measurement leaves something to be desired in the region of 7.8 MeV.

#### I.5 Re-measurement of the $^9\text{Be}(\gamma, n)$ Cross Section

Although the case of  $^9\text{Be}$  fits very well into our stated program of measuring the photoneutron cross sections for the 1p-shell nuclides, the real motivation for this measurement was provided by the publication of the results of a high resolution measurement of the  $^9\text{Be}(\gamma, n)$  cross section<sup>9)</sup>. This experimental result showed marked differences from many of the previous measurements, which were admittedly of coarse resolution. Because of this situation, a remeasurement was held to be desirable, and careful comparisons were made with other experiments.

Again, neutron yield curves were obtained as described above, but with one important modification. Because of the very low threshold for the  $^9\text{Be}(\gamma, n)^8\text{Be}$  reaction (1.67 MeV), the number of photoneutrons produced at low photon energies will be large enough to make it difficult to detect the increment in total neutron yield due to the stepping of the bremsstrahlung end-point energy. The ultimate result of producing too many photoneutrons at low photon energies is to decrease markedly the accuracy of the final cross section. Therefore, the number of low energy photons was diminished (and therefore the number of photoneutrons produced was diminished) by hardening the bremsstrahlung beam with 25 cm of carbon. The  $^9\text{Be}$  target was 9.2 gm/cm<sup>2</sup> of Be-metal.

The results of our measurement are shown in figures I.5.1. and I.5.2. The cross section, though it shows structure, is relatively unstructured when compared with that of Thomas et al<sup>9)</sup>. Figures I.5.3. and I.5.4. show the results of the present experiment compared with earlier results of Edge<sup>10)</sup>, Jakobson<sup>11)</sup>, Bertozzi et al<sup>12)</sup> for the low energy part of the cross section, and with the results of Nathans and Halpern<sup>13)</sup>, and of Costa et al<sup>14)</sup> over the total energy range. The comparison with the shell model calculations of Shackleton<sup>6)</sup> and of Majling et al<sup>15)</sup> is shown in figure I.5.5.



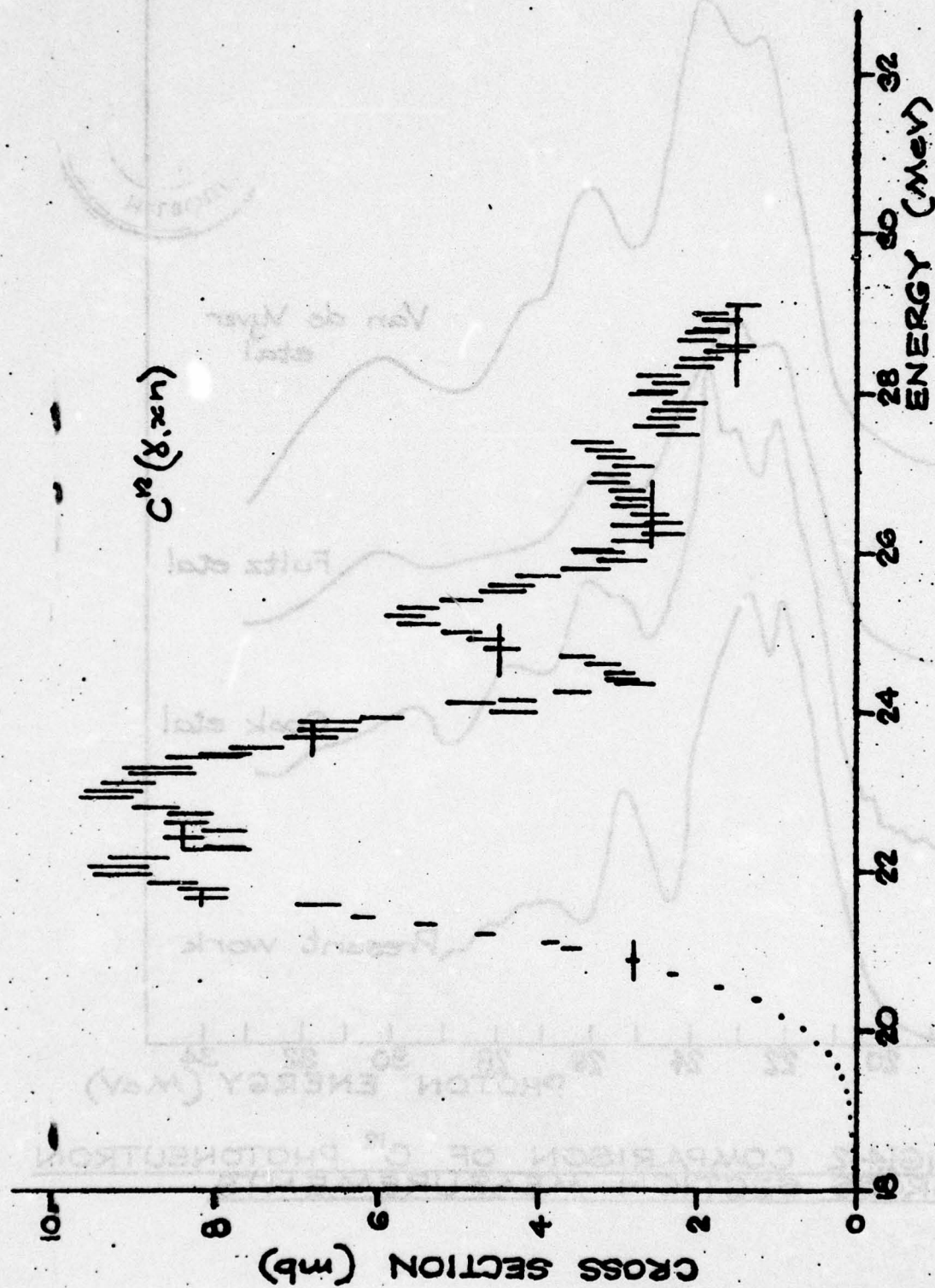


FIG. 4-1 CARBON-12 PHOTONEUTRON CROSS SECTION

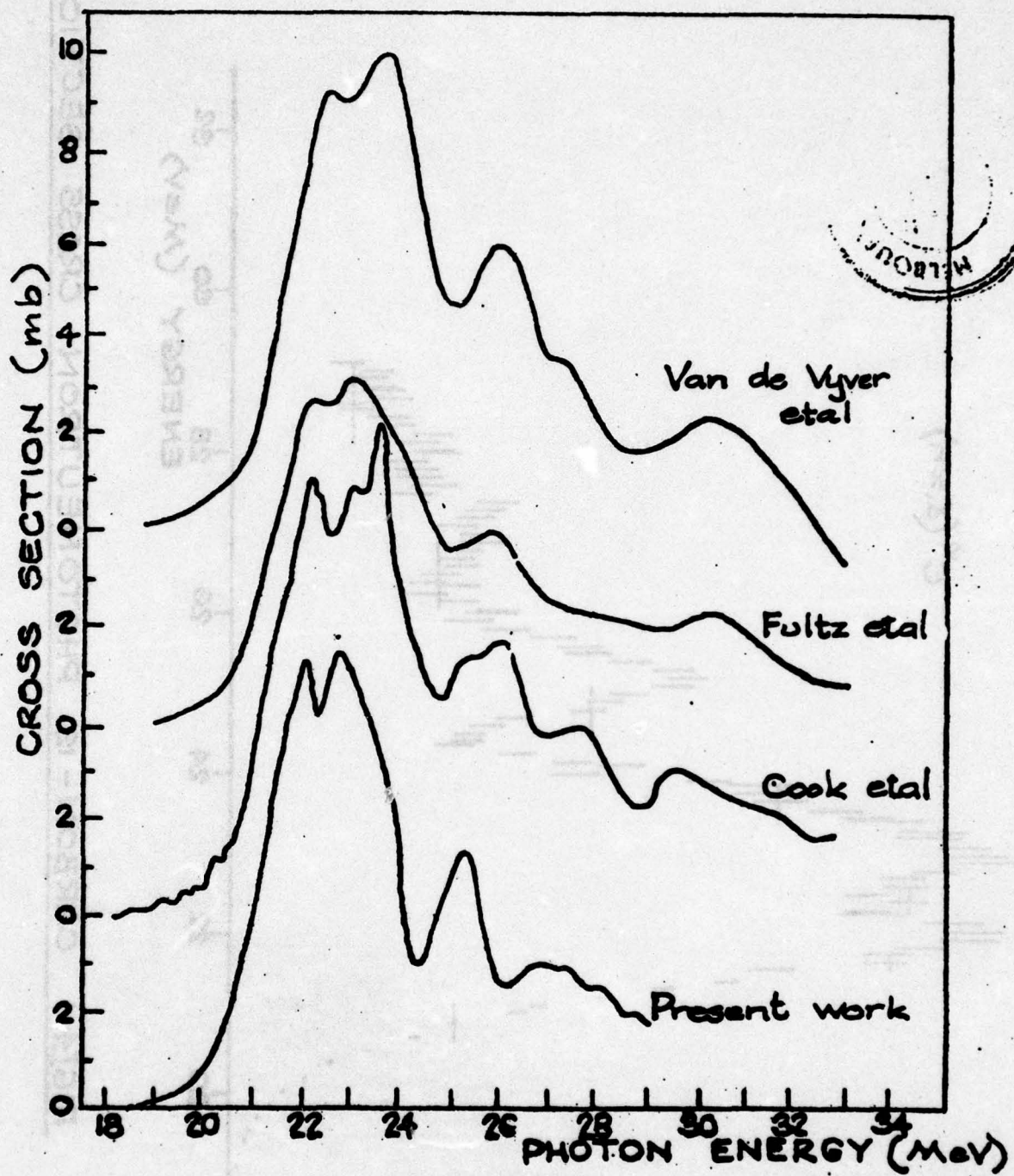


FIG 4-2 COMPARISON OF  $C^{12}$  PHOTONEUTRON CROSS SECTION MEASUREMENTS



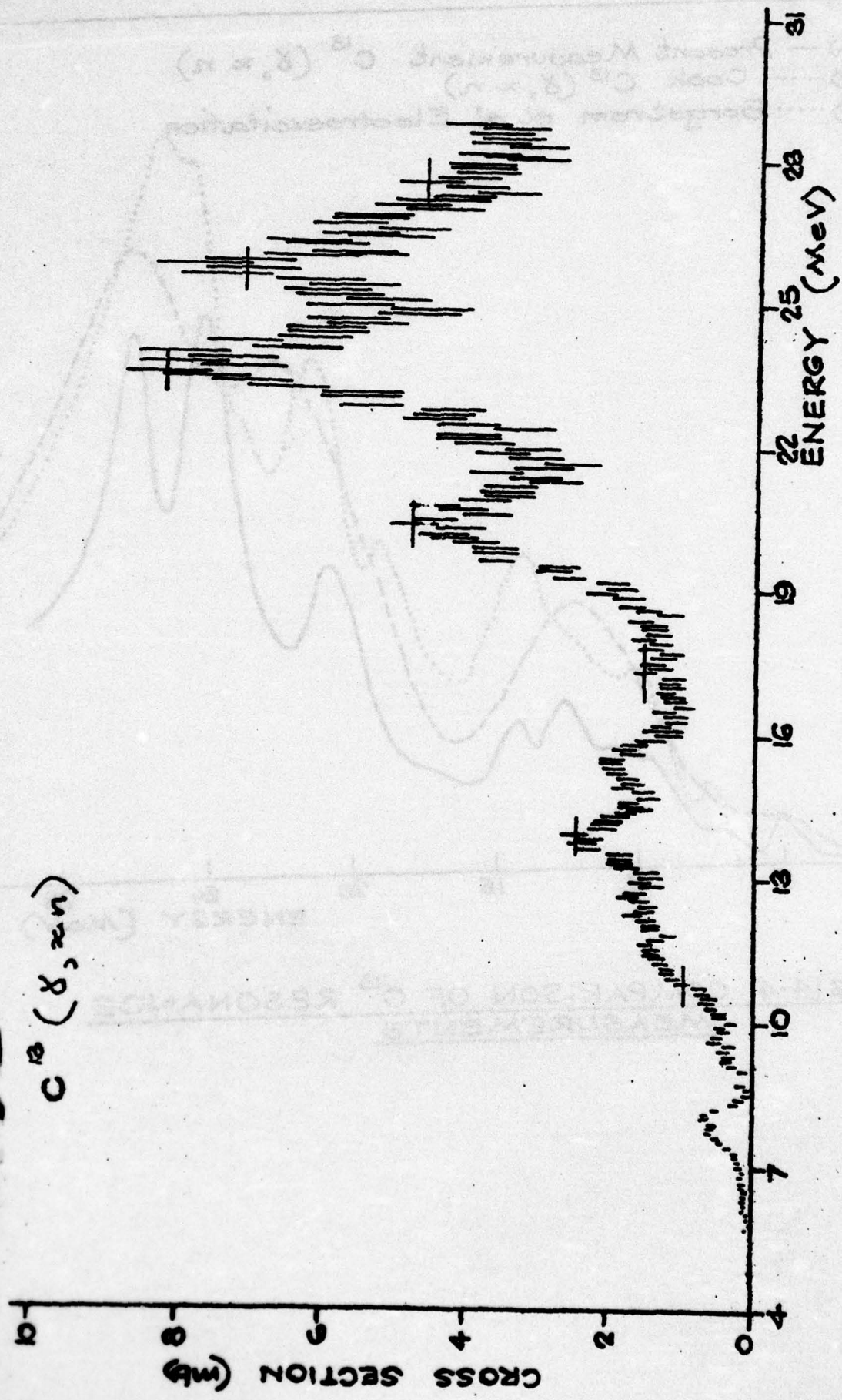


FIG.4-3 CARBON 13 PHOTONEUTRON CROSS SECTION

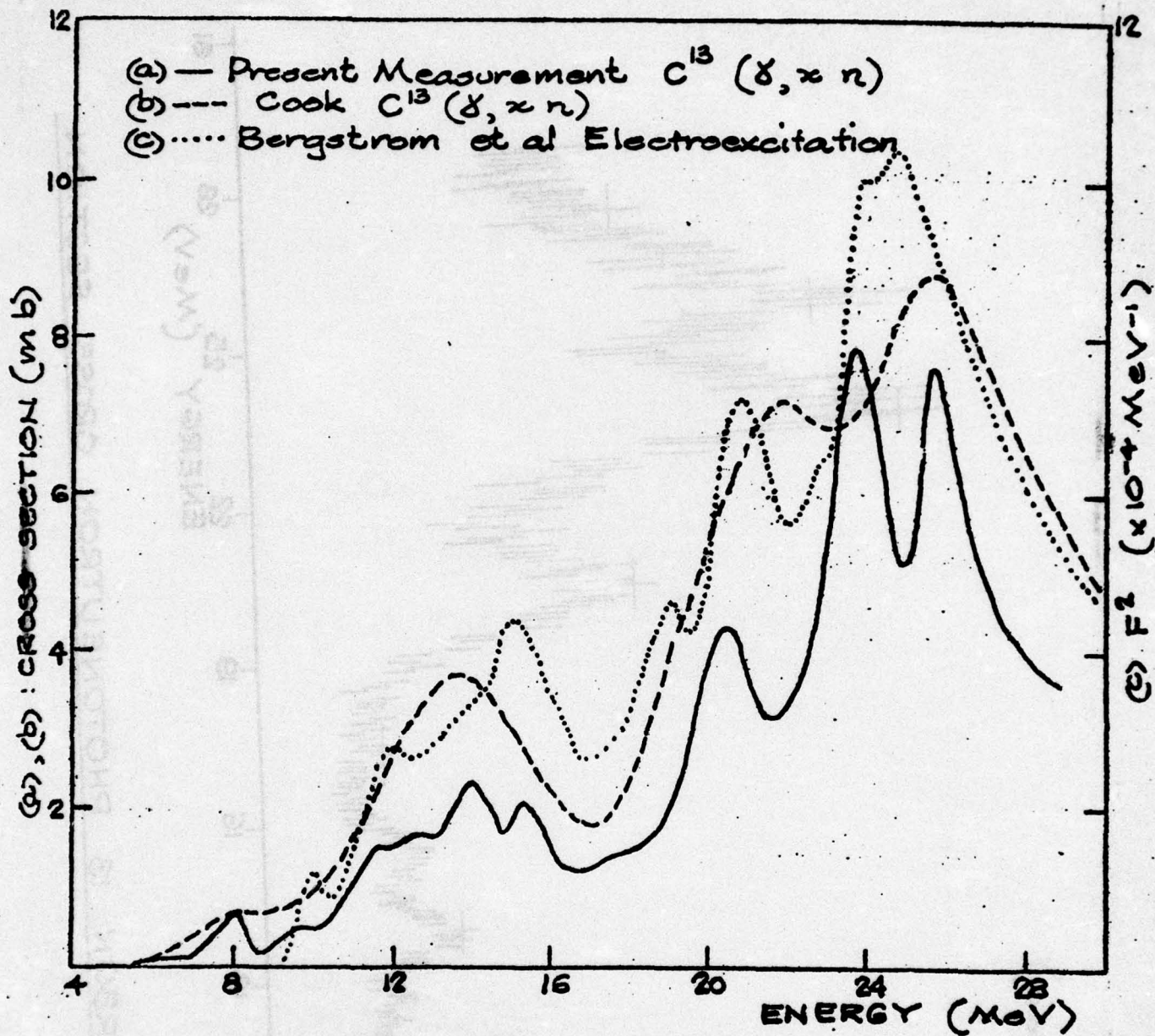
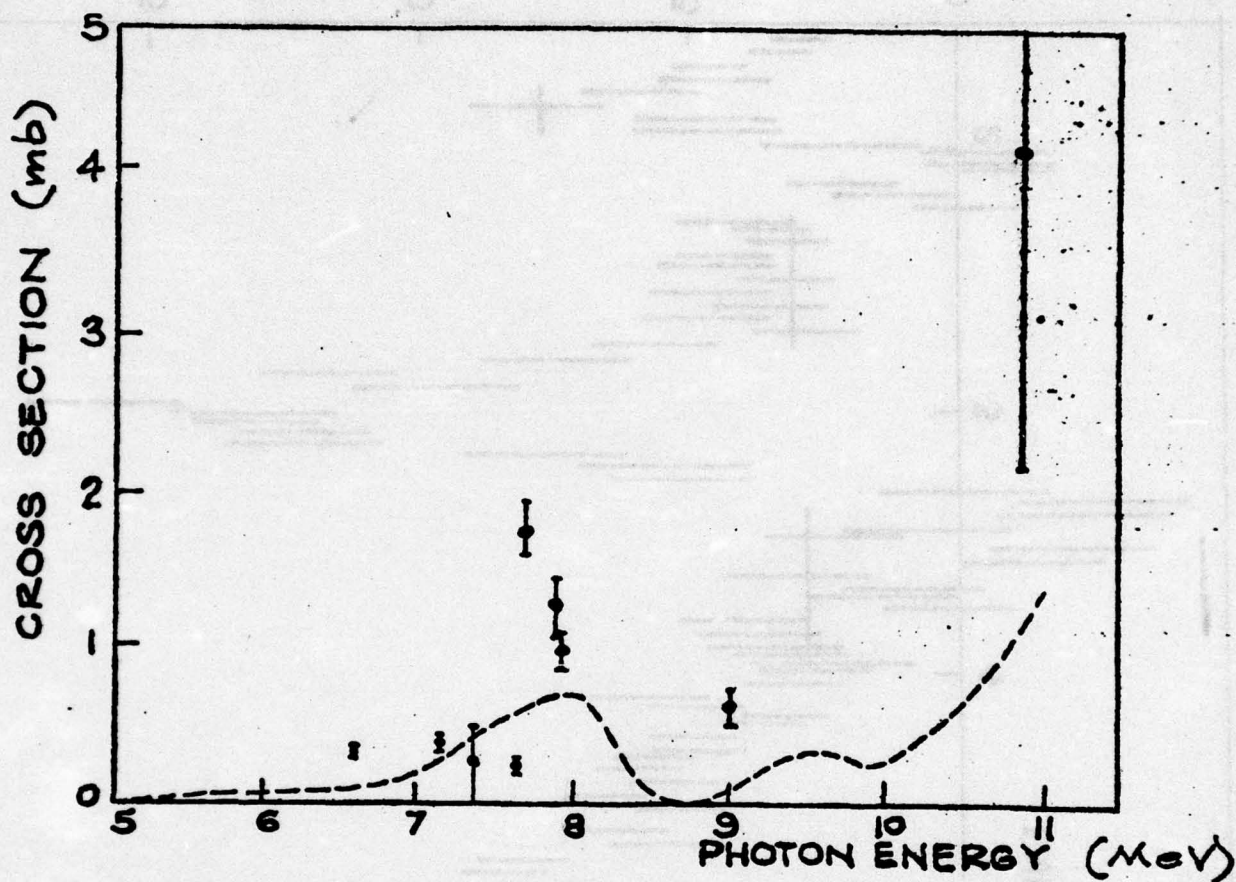


FIG 4-4 COMPARISON OF  $C^{13}$  RESONANCE MEASUREMENTS





I Green & Donahue  
 --- Present Measurement

FIG 4.5  $^{13}\text{C}(\gamma, n)$  CROSS SECTION

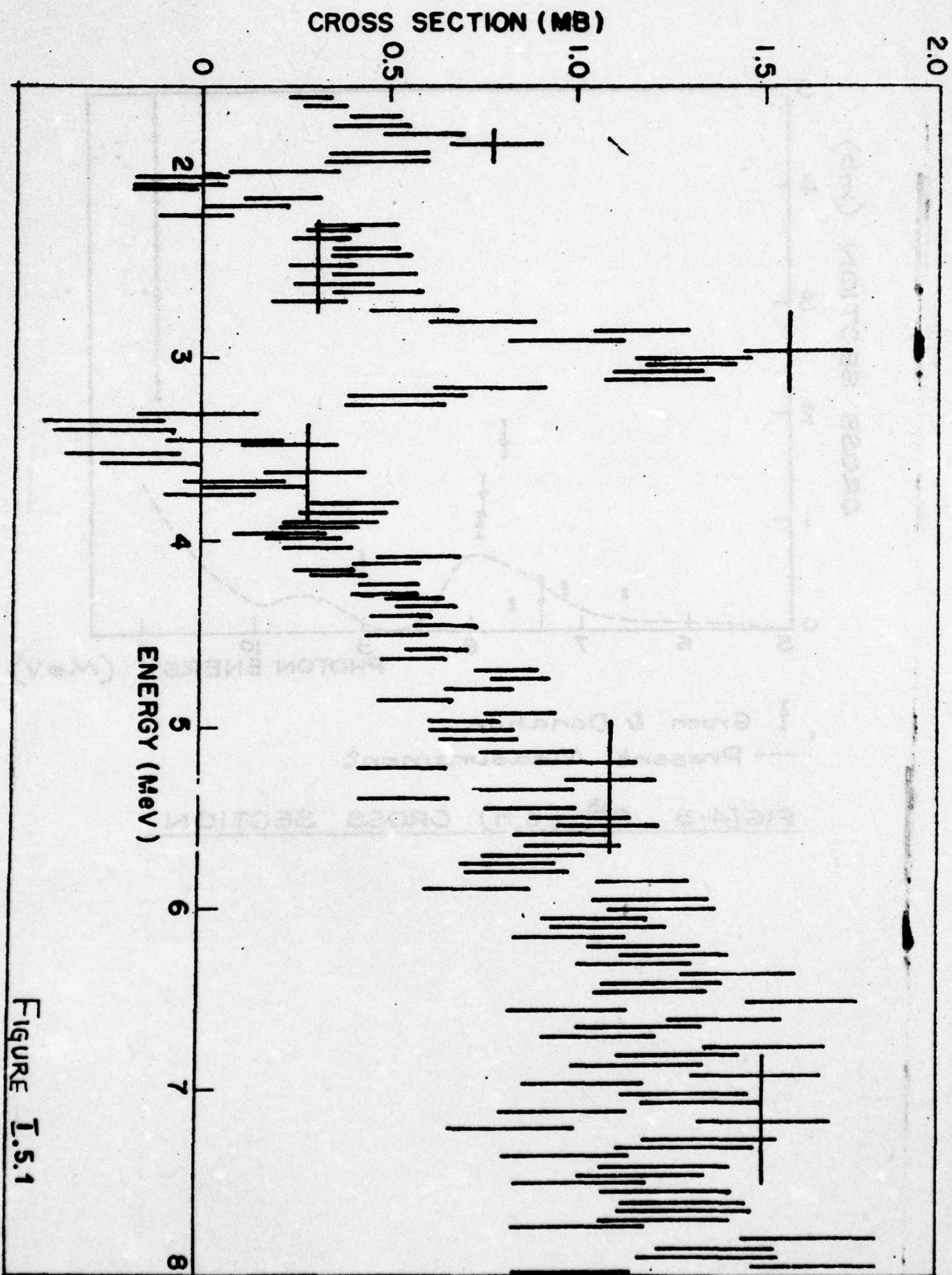


Figure I.5.1



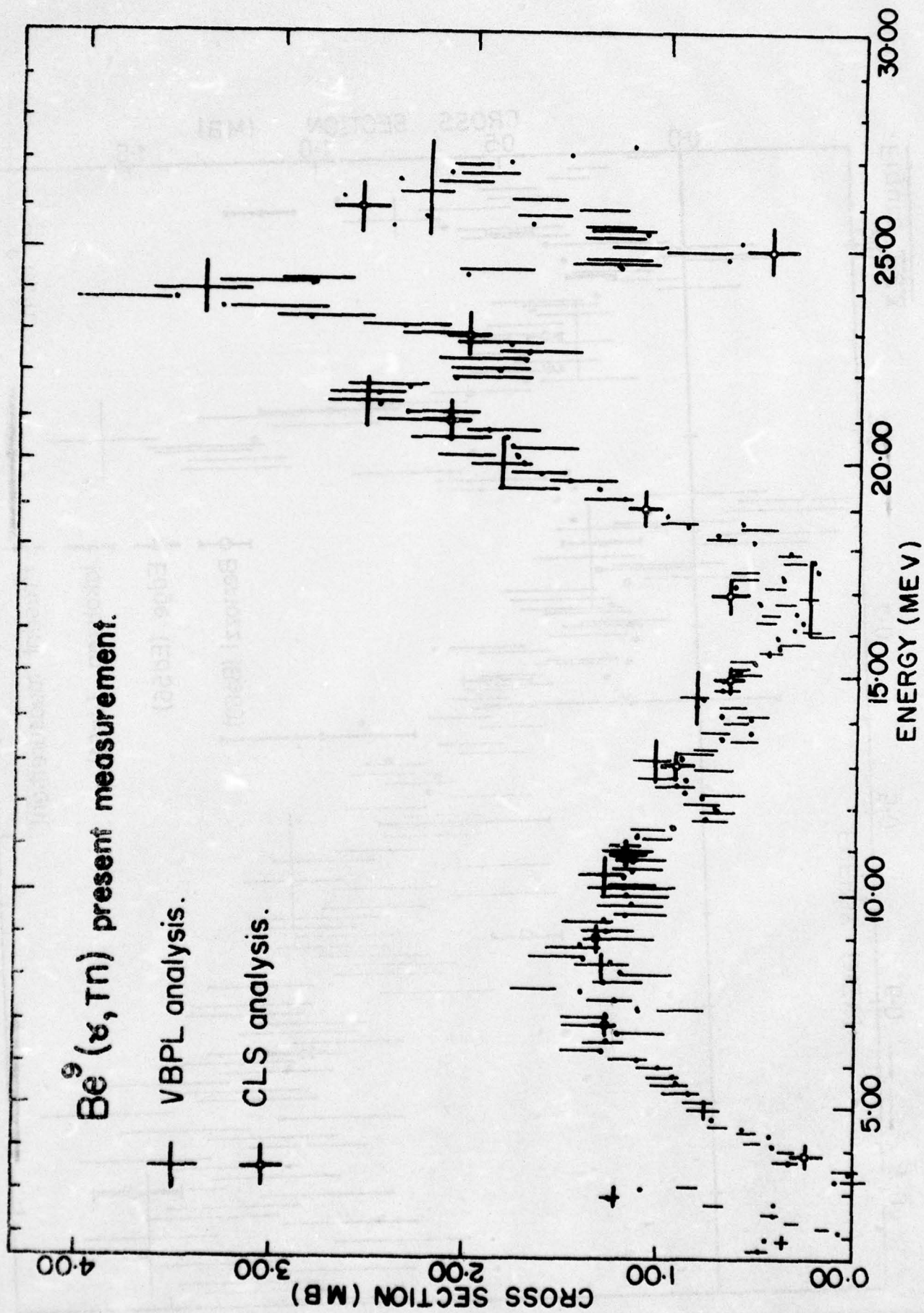


Figure I.5.2.

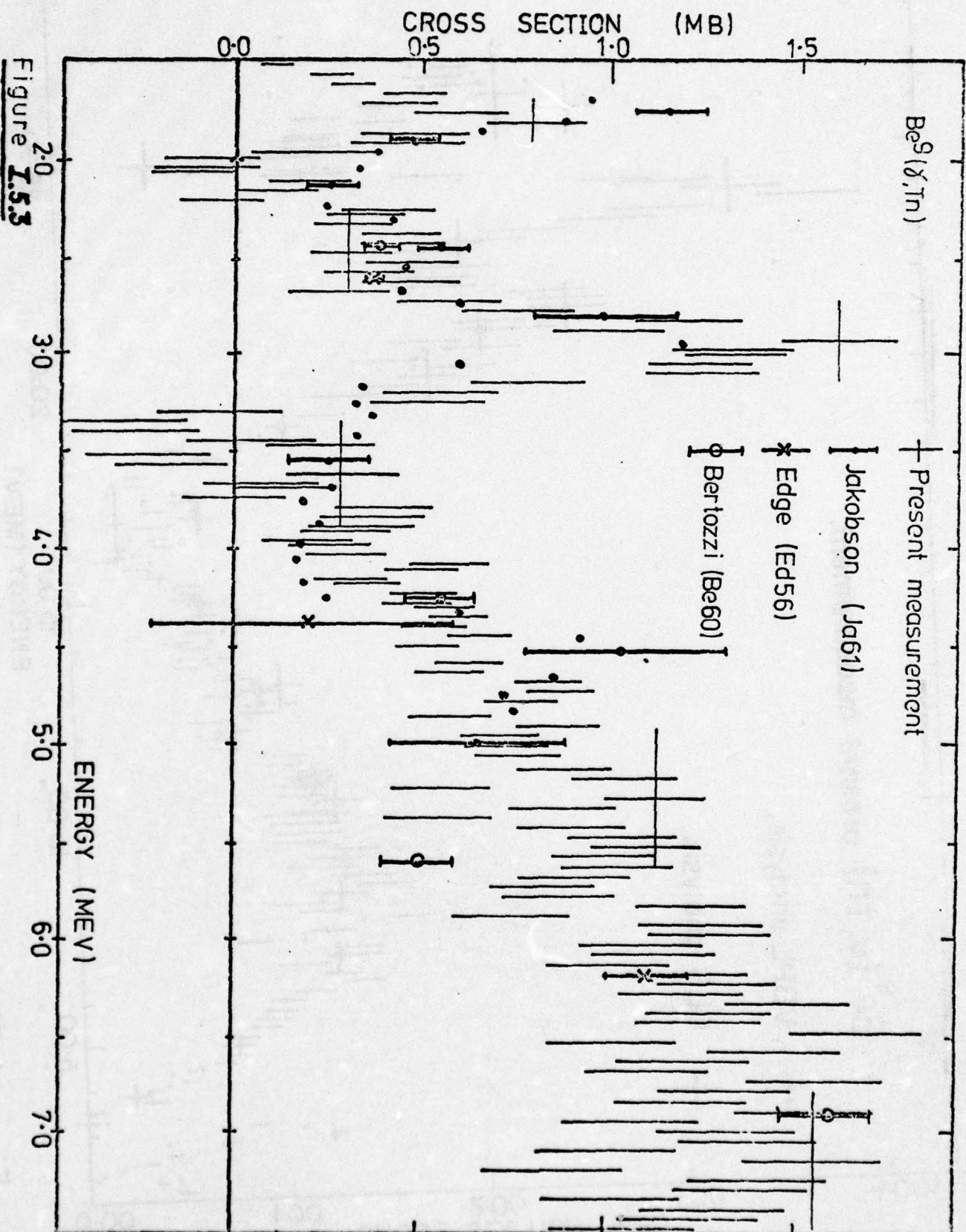


Figure 1.5.3



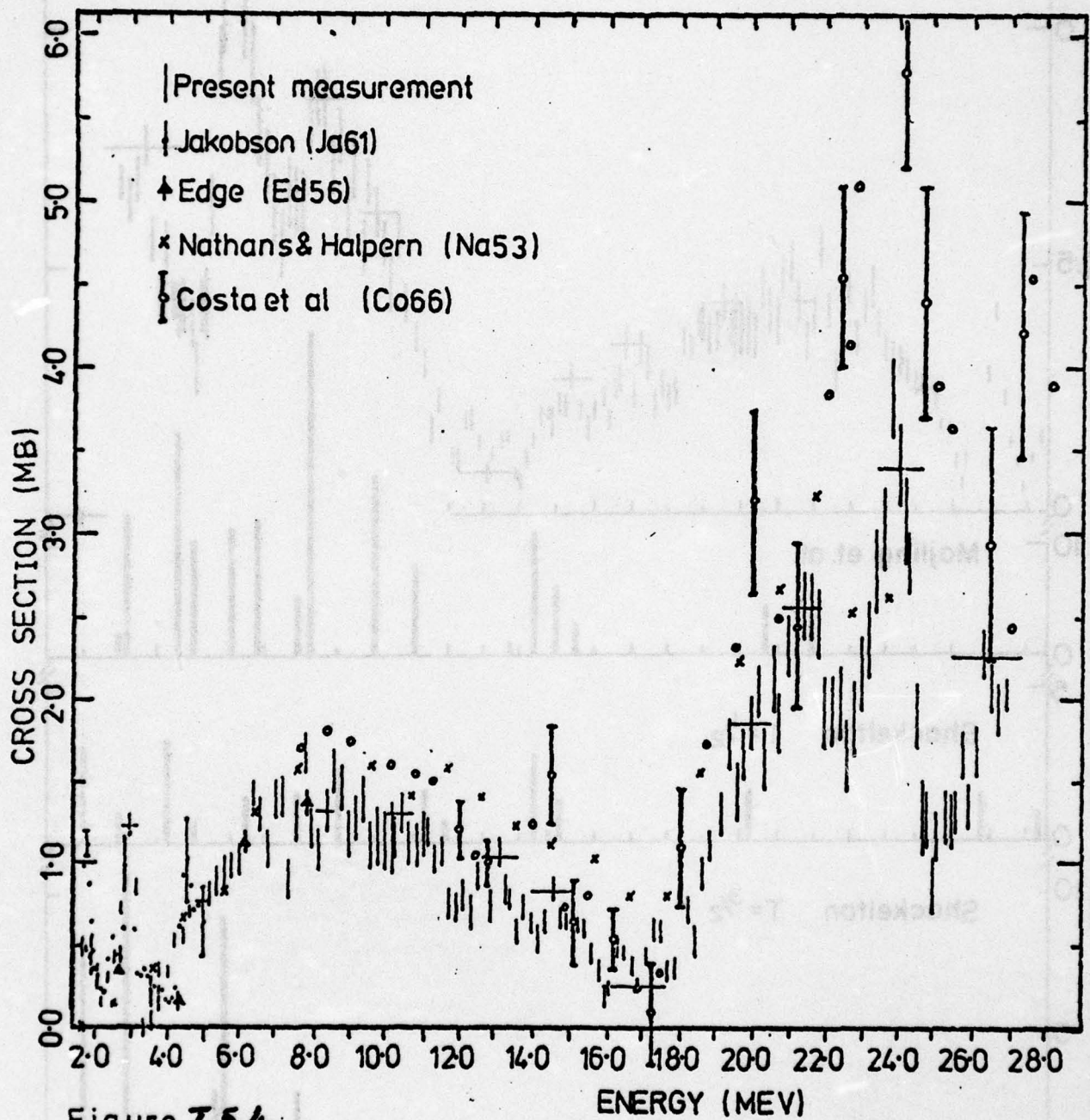


Figure I.5.4

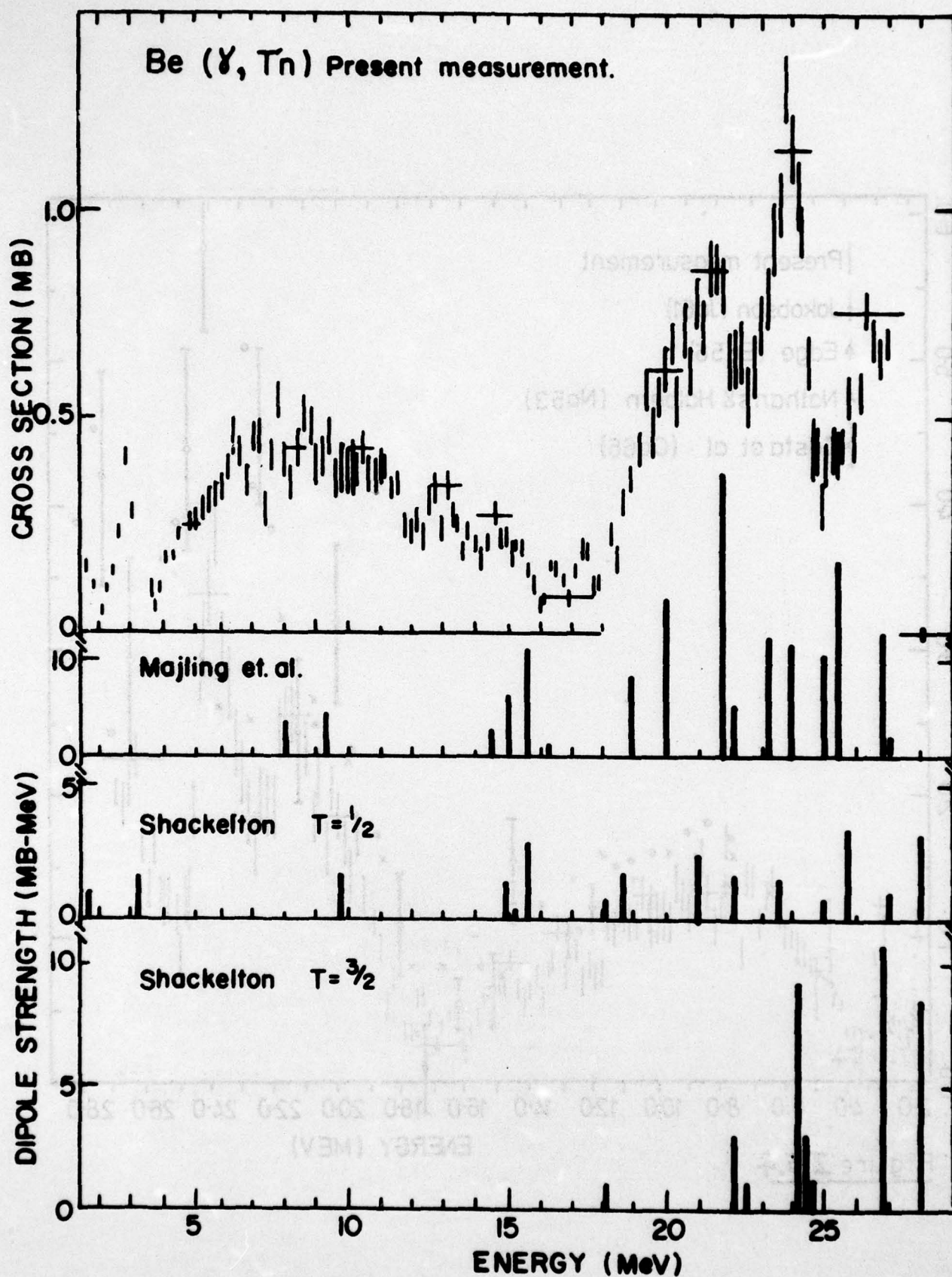


FIGURE I.5.5



## I.6 The Photoneutron Cross Section for Natural Osmium

The motivation for this study came from a private communication from Professor W. Greiner and collaborators (University of Frankfurt, W. Germany). On the basis of a series of studies of nuclear collective potential energy surfaces, they concluded that the osmium isotopes showed a transition from a strongly deformed axially symmetric nucleus ( $^{184}\text{Os}$ ) to a  $\gamma$ -unstable spherical vibrator ( $^{192}\text{Os}$ ), and they state that such a transition is the only case known to them. The potential energy surfaces for the osmium isotopes, as calculated, give a satisfactory fit to the low-lying energy level spectra, and a fairly good account of the inter- and intra-band  $\gamma$ -ray transition probabilities. Their calculations also predicted the shape of the giant dipole resonance for each of the isotopes.

Because of the extreme expense, and the unavailability for loan, of the separated osmium isotopes, the only test that could be made of the calculations of Greiner et al was a measurement of the photoneutron cross section of natural osmium.

The target for this experiment consisted of 20 gm of natural osmium, in powder form, enclosed in a plastic cylinder with thin mylar windows. An inert argon atmosphere was introduced into the cylinder to prevent any oxidation of the osmium. The naturally occurring osmium isotopes with their abundances are  $^{184}\text{Os}$  (0.02%),  $^{186}\text{Os}$  (1.59%),  $^{187}\text{Os}$  (1.64%),  $^{188}\text{Os}$  (13.3%),  $^{189}\text{Os}$  (16.1%),  $^{190}\text{Os}$  (26.4%) and  $^{192}\text{Os}$  (41.0%). Since the mass-190 and 192 isotopes dominate the relative abundance picture, it may be expected that these isotopes will also be dominant factors in any comparison of the shape of the giant dipole resonance.

The yield curve of photoneutrons from natural osmium was measured, and analysed to give  $\sigma(\gamma, \text{Tn})$  for natural osmium. This cross section is shown in figure I.6.1. The most important characteristic of this cross section is its narrow width of about 5 MeV. This occurs in spite of the expected broadening due to the presence of many isotopes in the target, and due to the predicted deformation of some of them. A private communication from Professor Greiner gave as the prediction of the theory, with the contributions of all the isotopes included and weighted according to their abundances, the full line shown in figure I.6.1.

It is unfortunate that the separated osmium isotopes were not available for hire at the time of these experiments for it would have been very interesting to trace, through the changing shape of the giant resonances, the changing potential energy surfaces of these isotopes.

## II. ( $\gamma, p$ ) AND ( $e, e'p$ ) STUDIES

### II.1 Photoprotons from $^{90}\text{Zr}$ , $^{91}\text{Zr}$ and $^{92}\text{Zr}$

This work began with an attempt to find structure in the spectrum of photoprotons from  $^{90}\text{Zr}$ . Such structure had been quite strongly suggested in a study of the inverse reaction  $^{89}\text{Y}(p, \gamma_0)^{90}\text{Zr}$  carried out by Hasinoff et al<sup>22)</sup> at Stanford University. Measurements of the photoproton spectra from both  $^{90}\text{Zr}$  and  $^{91}\text{Zr}$  targets were made using 30 MeV bremsstrahlung from the Melbourne betatron. These are shown in figure II.1.1. The identification of the various peaks in the proton spectrum from  $^{90}\text{Zr}$  as either proton groups which left  $^{89}\text{Y}$  in its ground state - or excited states - was made at Tohoku University, Japan, in collaboration with Professor K. Shoda. The identification of the emitting states as  $T_<$  or  $T_>$  giant resonance states has also been established in the series of measurements of proton spectra from the ( $e, e'p$ )

# NATURAL OSMIUM

$$\sigma(\gamma, n) + \sigma(\gamma, 2n) + \sigma(\gamma, 3n) + \sigma(\gamma, np)$$

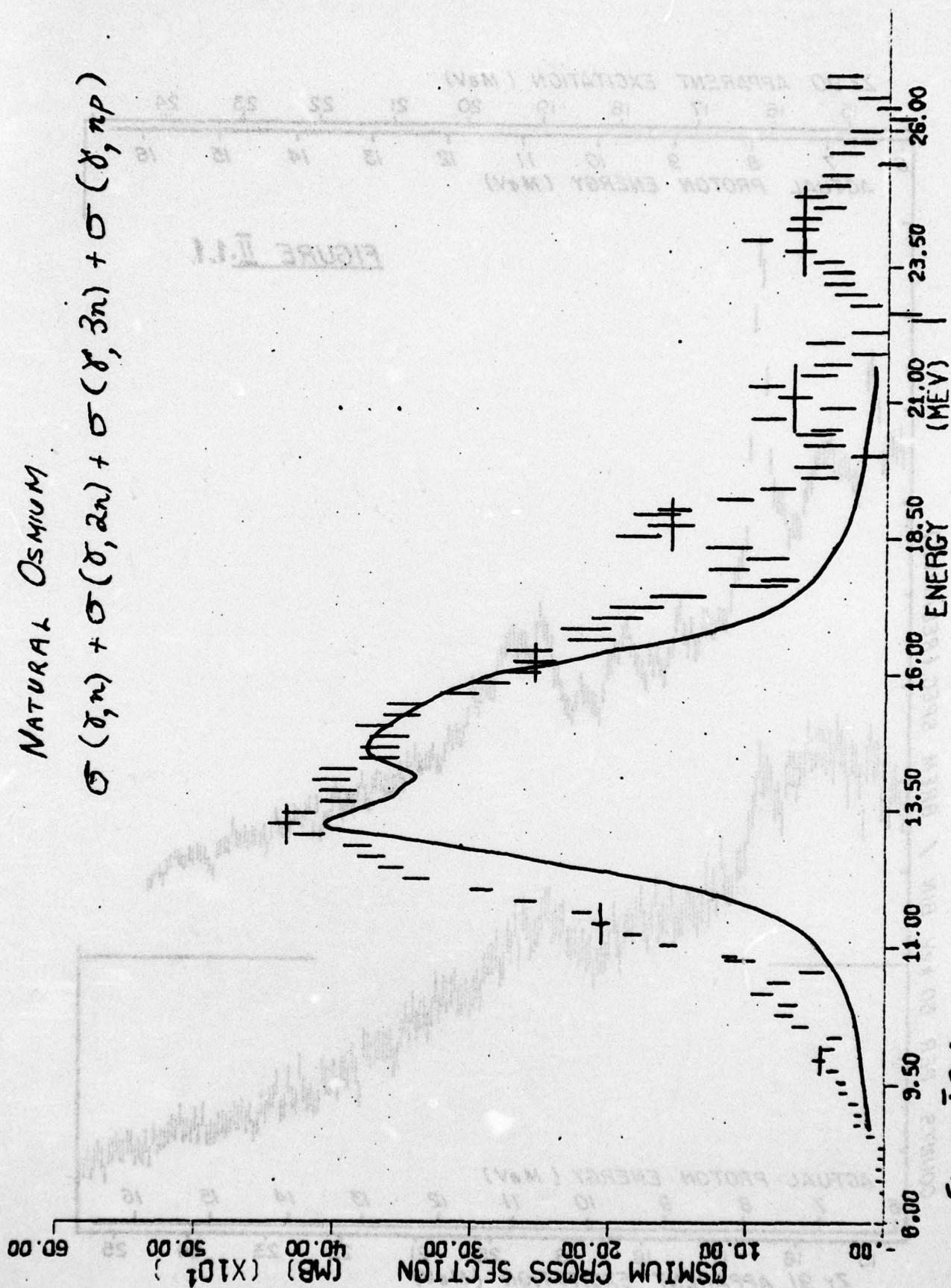
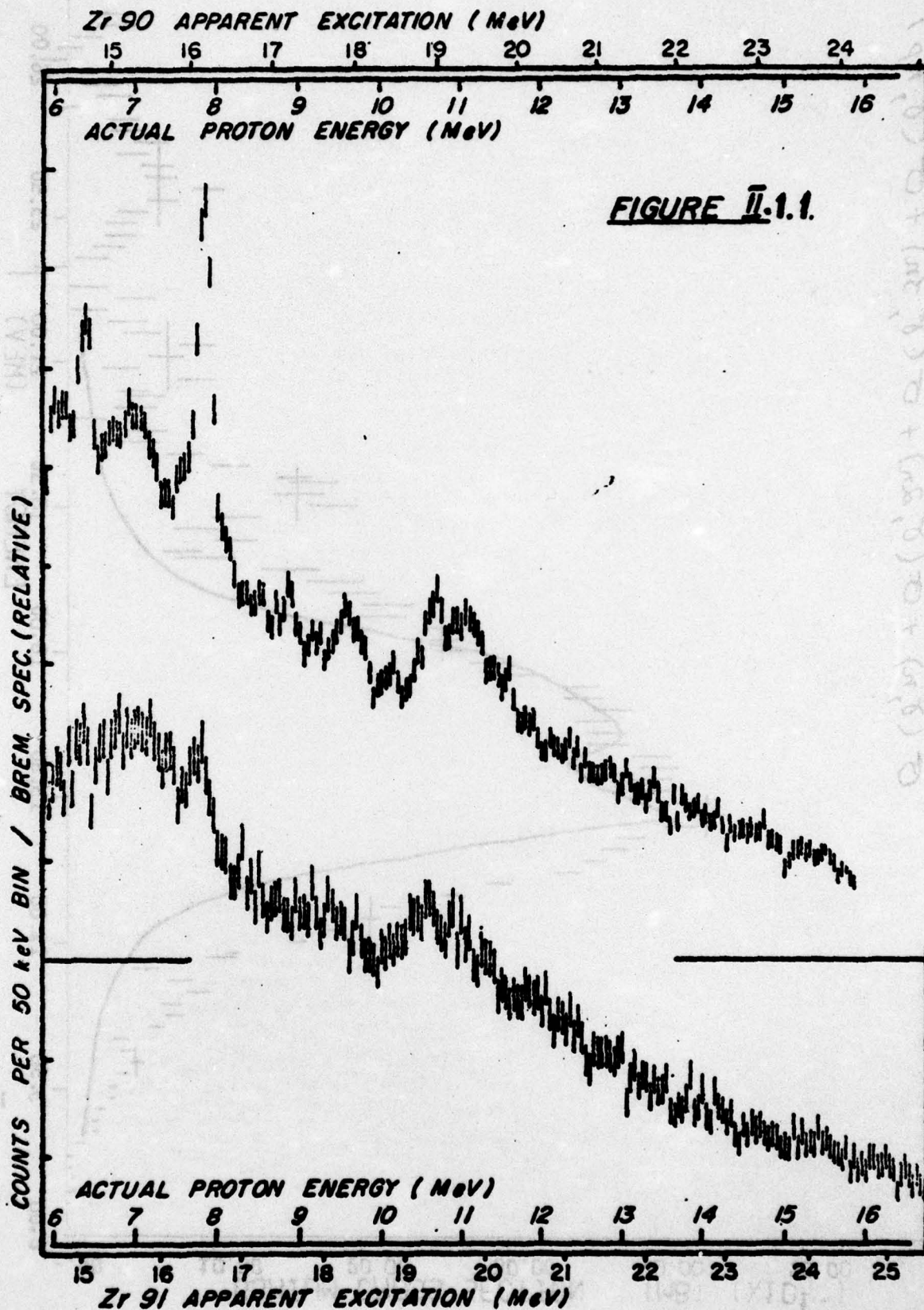


Figure 16.1.





reaction at various electron energies.

A detailed correspondence of proton groups in the spectra from  $^{90}\text{Zr}$  and  $^{91}\text{Zr}$  was established, particularly for the region of proton energies between 9.5 and 12 MeV. In  $^{90}\text{Zr}$ , this structure has been shown to represent absorption strength into  $T = 6$  ( $T_2$ ) electric dipole states.

The weak coupling core-excitation model accounts for the structure in the photoproton spectra from  $^{91}\text{Zr}$  by means of the postulate that the structure represents  $T = 13/2$  ( $T_2$ ) absorption strength, formed by the coupling of  $1^-$ ,  $T=6$   $^{90}\text{Zr}$  core states to the spectator neutron, which is in a  $2d_{5/2}$  single particle state. This is consistent with the experimental findings, and also with current models for the low-lying  $^{90}\text{Y}$  states, which are regarded as  $^{89}\text{Y}$ -core states coupled to a  $2d_{5/2}$  single neutron.

This model is currently being tested further in the measurement of proton spectra from the electrodisintegration of  $^{92}\text{Zr}$ . Preliminary results indicate that the core excitation model is not now applicable, possibly due to the strength of the pairing force between the two last-added neutrons in  $^{92}\text{Zr}$ .

### III. DE-EXCITATION $\gamma$ -RAY MEASUREMENTS

#### III.1 De-excitation $\gamma$ -ray spectra in $^{19}\text{F}$ , $^{31}\text{P}$ , and $^{39}\text{K}$ targets

Spectra of  $\gamma$ -rays emitted following the photodisintegration of  $^{19}\text{F}$ ,  $^{31}\text{P}$  and  $^{39}\text{K}$  have been measured, in the case of the fluorine target for a number of bremsstrahlung end-point energies. This latter situation has enabled estimates to be made of the energy variation of the cross section for emission of the two most prominent  $\gamma$ -rays. These are the  $\gamma$ -rays from the transition from the 1.98 MeV state to ground in  $^{18}\text{O}$  (following a  $(\gamma, p)$  reaction), and the transition from the 5.3 MeV doublet (spins  $5/2^+$  and  $1/2^+$ ) to ground in  $^{15}\text{N}$  (following a  $(\gamma, \alpha)$  reaction). The cross section for the  $(\gamma, p_1)$  reaction rose from threshold (8 MeV) and from 14 MeV to 28 MeV stayed constant (within about 25%). On the other hand, the  $(\gamma, \alpha_1 2)$  reaction cross section rose relatively slowly from threshold (4 MeV) to a peak at 15 MeV, then falling off relatively rapidly to zero at about 20 MeV.

In the cases of  $^{31}\text{P}$  and  $^{39}\text{K}$  targets, spectra of de-excitation  $\gamma$ -rays have been measured with bremsstrahlung of end-point energy 30 MeV, and the final states populated have been noted. In the case of  $^{31}\text{P}$ , it has been shown that the large  $(\gamma, \alpha)$  contribution reported previously by the Toronto group is due to  $\gamma$ -rays following the inelastic scattering of neutrons in the aluminium casing of the Ge(Li) detector used to measure the  $\gamma$ -ray spectra.

For  $^{31}\text{P}$  and  $^{39}\text{K}$ , a Tamm-Dancoff type shell model calculation, which has previously had reasonable success in predicting the total giant dipole resonance absorption strength for several  $A = 4n-1$  nuclides, has been extended to predict the total and partial photoneutron and photoproton cross sections of the  $^{39}\text{K}$  and  $^{31}\text{P}$  nuclei.

An initial simplified calculation to predict cross sections of particular reactions in  $^{31}\text{P}$ , leaving specified residual states in  $^{30}\text{P}$  and  $^{30}\text{Si}$  was in good agreement with the population of final states as measured in the de-excitation  $\gamma$ -ray spectrum.

Total photoneutron yield curves for both  $^{31}\text{P}$  and  $^{39}\text{K}$  have been measured and are being analysed to give the  $(\gamma, n)$  cross sections. Final assessment of the theoretical calculations against all available experimental information is



reaction at various electron energies.

A detailed correspondence of proton groups in the spectra from  $^{90}\text{Zr}$  and  $^{91}\text{Zr}$  was established, particularly for the region of proton energies between 9.5 and 12 MeV. In  $^{90}\text{Zr}$ , this structure has been shown to represent absorption strength into  $T = 6$  ( $T_2$ ) electric dipole states.

The weak coupling core-excitation model accounts for the structure in the photoproton spectra from  $^{91}\text{Zr}$  by means of the postulate that the structure represents  $T = 13/2$  ( $T_2$ ) absorption strength, formed by the coupling of  $1^-$ ,  $T=6$   $^{90}\text{Zr}$  core states to the spectator neutron, which is in a  $2d_{5/2}$  single particle state. This is consistent with the experimental findings, and also with current models for the low-lying  $^{90}\text{Y}$  states, which are regarded as  $^{89}\text{Y}$ -core states coupled to a  $2d_{5/2}$  single neutron.

This model is currently being tested further in the measurement of proton spectra from the electrodisintegration of  $^{92}\text{Zr}$ . Preliminary results indicate that the core excitation model is not now applicable, possibly due to the strength of the pairing force between the two last-added neutrons in  $^{92}\text{Zr}$ .

### III. DE-EXCITATION $\gamma$ -RAY MEASUREMENTS

#### III.1 De-excitation $\gamma$ -ray spectra in $^{19}\text{F}$ , $^{31}\text{P}$ , and $^{39}\text{K}$ targets

Spectra of  $\gamma$ -rays emitted following the photodisintegration of  $^{19}\text{F}$ ,  $^{31}\text{P}$  and  $^{39}\text{K}$  have been measured, in the case of the fluorine target for a number of bremsstrahlung end-point energies. This latter situation has enabled estimates to be made of the energy variation of the cross section for emission of the two most prominent  $\gamma$ -rays. These are the  $\gamma$ -rays from the transition from the 1.98 MeV state to ground in  $^{18}\text{O}$  (following a  $(\gamma, p)$  reaction), and the transition from the 5.3 MeV doublet (spins  $5/2^+$  and  $1/2^+$ ) to ground in  $^{15}\text{N}$  (following a  $(\gamma, \alpha)$  reaction). The cross section for the  $(\gamma, p_1)$  reaction rose from threshold (8 MeV) and from 14 MeV to 28 MeV stayed constant (within about 25%). On the other hand, the  $(\gamma, \alpha_1 2)$  reaction cross section rose relatively slowly from threshold (4 MeV) to a peak at 15 MeV, then falling off relatively rapidly to zero at about 20 MeV.

In the cases of  $^{31}\text{P}$  and  $^{39}\text{K}$  targets, spectra of de-excitation  $\gamma$ -rays have been measured with bremsstrahlung of end-point energy 30 MeV, and the final states populated have been noted. In the case of  $^{31}\text{P}$ , it has been shown that the large  $(\gamma, \alpha)$  contribution reported previously by the Toronto group is due to  $\gamma$ -rays following the inelastic scattering of neutrons in the aluminium casing of the Ge(Li) detector used to measure the  $\gamma$ -ray spectra.

For  $^{31}\text{P}$  and  $^{39}\text{K}$ , a Tamm-Dancoff type shell model calculation, which has previously had reasonable success in predicting the total giant dipole resonance absorption strength for several  $A = 4n-1$  nuclides, has been extended to predict the total and partial photoneutron and photoproton cross sections of the  $^{39}\text{K}$  and  $^{31}\text{P}$  nuclei.

An initial simplified calculation to predict cross sections of particular reactions in  $^{31}\text{P}$ , leaving specified residual states in  $^{30}\text{P}$  and  $^{30}\text{Si}$  was in good agreement with the population of final states as measured in the de-excitation  $\gamma$ -ray spectrum.

Total photoneutron yield curves for both  $^{31}\text{P}$  and  $^{39}\text{K}$  have been measured and are being analysed to give the  $(\gamma, n)$  cross sections. Final assessment of the theoretical calculations against all available experimental information is still awaited.

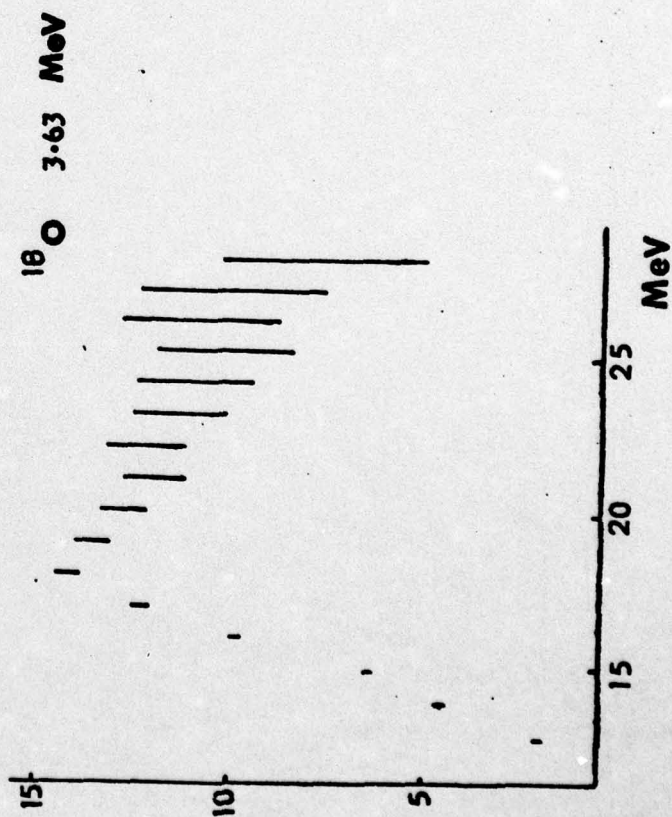
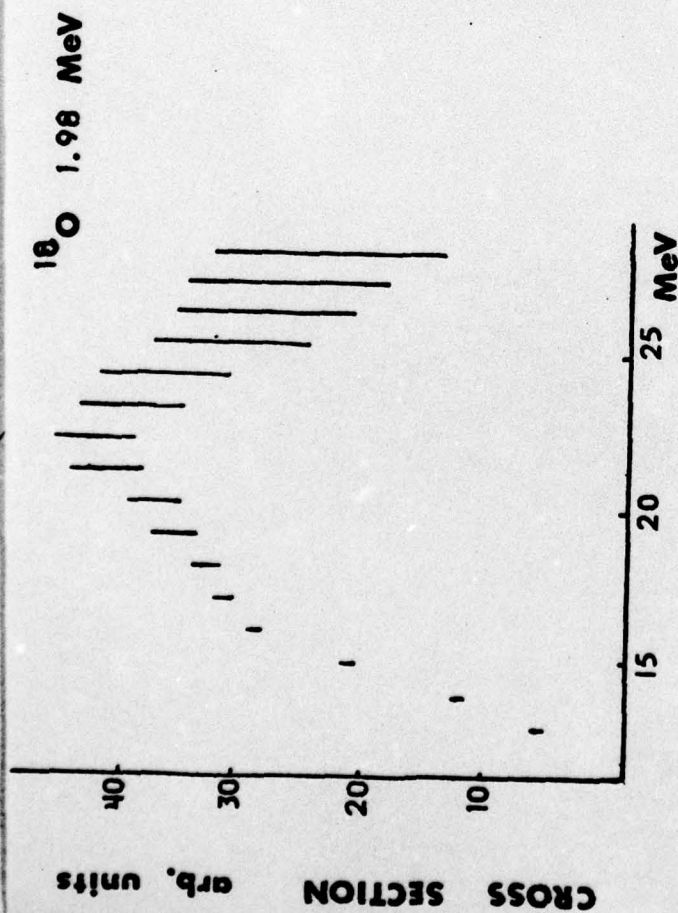
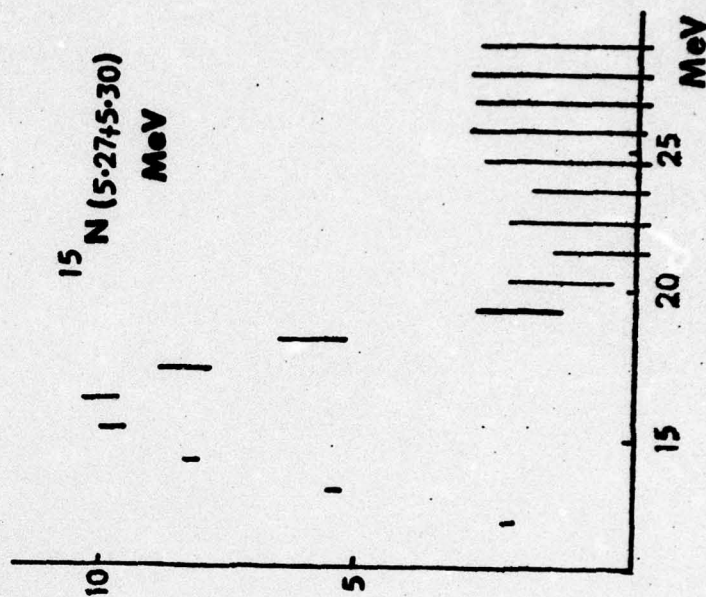
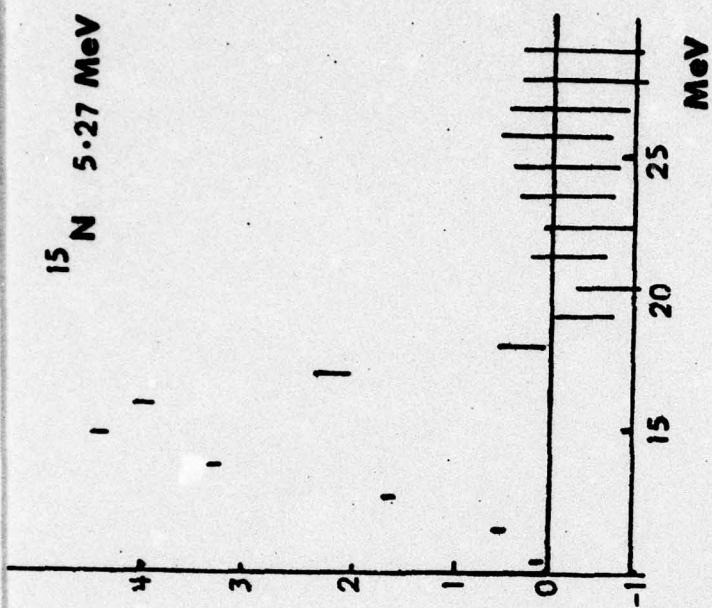


FIGURE III.1.1



#### IV. K-SHELL IONIZATION BY RELATIVISTIC ELECTRONS

##### IV.1 K-ionization cross sections in Ni, Ag and Au

The experiment in which the energy variation of the total K-shell ionization cross section was measured between 3 and 30 MeV was completed in a previous grant period (1972). Consequently, the work done in the present grant period has been concerned with the calculation of small corrections to the experimental results, and to the interpretation of the final results. Two papers have now been published on this work.

## REFERENCES

1. E. Bramanis, T. K. Deague, R. S. Hicks, R. J. Hughes, E. G. Muirhead, R. H. Sambell and R.J.J. Stewart  
Nuclear Instruments and Methods 100 (1972) 59-71.
2. F. B. Malik and W. Scholz, Phys.Rev. 150 (1966) 971  
W. Scholz and F. B. Malik, Phys.Rev. 153 (1966) 1071.
3. J. M. Blatt and V. F. Weisskopf, "Theoretical Nuclear Physics"  
John Wiley and Sons, New York (1952).
4. M. Danos, Nuclear Physics 5 (1958) 23  
K. Okamoto, Phys.Rev. 110 (1958) 143.
5. S. Oikawa, Ph.D. thesis, Tohoku University (1974).  
See also K. Shoda, A series of lectures on Nuclear Isospin (University of Melbourne, April 1974) - unpublished.
6. R. Shackleton, Ph.D. thesis, University of Melbourne (1971) unpublished.
7. B. M. Spicer and R. F. Fraser, Aust.J.Phys. 26 (1973) 7.
8. I. V. Kurdyumov and Yu. F. Smirnov, Vestnik M.G.U. 4 (1968) 104.
9. B. W. Thomas, D. M. Crawford and H. H. Thies, Nuclear Physics A196 (1972) 89.
10. R. D. Edge, Nuclear Physics 2 (1956) 485.
11. M. K. Jakobson, Phys.Rev. 123 (1961) 229.
12. W. Bertozzi, P. T. Demos, C. P. Sargent, W. Turchinets, D. B. McConnell and S. Kowalski, Karlsruhe Conference on Photonuclear Reactions (1960).
13. R. Nathans and J. Halpern, Phys.Rev. 92 (1953) 940.
14. S. Costa, L. Pasqualini, G. Piragino and L. Roasio, Nuovo Cimento B42 (1966) 306.
15. L. Majling, V. I. Kukulín and Yu. F. Smirnov, Czech.J.Phys. B18 (1968) 1560.
16. B. C. Cook, J.E.E. Baglin, J. N. Bradford and J. E. Griffin, Phys.Rev. 143 (1966) 724.
17. S. C. Fultz, J. T. Caldwell, B. L. Berman, R. L. Bramblett and R.R. Harvey, Phys.Rev. 143 (1966) 790.
18. R. E. Van de Vyver, H. Ferdinance, G. Kruyt, R. Carchon and R. Devos, Nuclear Physics A198 (1972) 144.
19. B. C. Cook, Phys.Rev. 106 (1957) 300.
20. J. G. Bergstrom, H. Crannell, F. J. Kline, J. T. O'Brien, J. W. Lightbody and S. P. Fivozinsky, Phys.Rev. C4 (1971) 1514.
21. L. Green and D. J. Donahue, Phys.Rev. 135 (1964) B701.
22. M. Hasinoff, G. A. Fisher, H. M. Kuan and S. S. Hanna, Physics Letters 30B (1969) 337.



## APPENDIX 1

### List of Papers Published

1. B. M. Spicer and R. F. Fraser  
"The Dipole States of Mass-11 Nuclei"  
Australian Journal of Physics 26 (1973) 7 - 16.
2. K.J.F. Allen and A. G. Klein  
"A Technique for the Correction of Pulse Heights from Thick Silicon Particle Detectors"  
Nuclear Instruments and Methods 108 (1973) 309 - 315.
3. H. J. Askin, R. S. Hicks, K.J.F. Allen, R. J. Petty and M. N. Thompson  
"Isobaric Spin Mixing in the Analog States of  $^{90}\text{Zr}$ "  
Nuclear Physics A204 (1973) 209 - 219.
4. R. H. Sambell and B. M. Spicer  
"The Photoneutron Cross Section of  $^{45}\text{Sc}$ "  
Nuclear Physics A205 (1973) 139 - 144.
5. R. S. Hicks and B. M. Spicer  
"The Dynamic Collective Model Interpretation of the Photoneutron Cross Section of  $^{181}\text{Ta}$ "  
Australian Journal of Physics 26 (1973) 585 - 595.
6. B. M. Spicer  
"An Interpretation of De-excitation Gamma Ray Spectra Measurements following the Photodisintegration of  $^{12}\text{C}$ ,  $^{16}\text{O}$  and  $^{40}\text{Ca}$ "  
Australian Journal of Physics 26 (1973) 269 - 277.
7. G. R. Dangerfield  
"K-Shell Ionization by Extreme Relativistic Electrons"  
Physics Letters 46A (1973) 19 - 20.
8. R. J. Hughes and E. G. Muirhead  
"The Photoneutron Cross Sections of  $^{10}\text{B}$  and  $^{11}\text{B}$ "  
Nuclear Physics A215 (1973) 147 - 156.
9. Judith M. Dixon and M. N. Thompson  
"The Effect of Excited State Decays on the Measured Angular Distribution of the  $^{12}\text{C}(\gamma, p)^{11}\text{B}$  Reaction"  
Australian Journal of Physics 27 (1974) 301 - 306.
10. R. J. Hughes, R. H. Sambell, E. G. Muirhead and B. M. Spicer  
"The Photoneutron Cross Section of  $^9\text{Be}$ "  
Nuclear Physics A238 (1975) 189 - 198.
11. G. R. Dangerfield and B. M. Spicer  
"K-Shell Ionization by Relativistic Electrons"  
Journal of Physics B 8 (1975) 1744.

List of Papers presented at Meetings

## Conference on "Nuclear Structure Studies using Electron Scattering and Photoreaction"

Sendai, Japan, September 12 - 15, 1972

Paper IV-E - Cross Sections for  $^{32}\text{S}(\gamma, n)^{31}\text{S}^*$  and  $^{32}\text{S}(\gamma, p)^{31}\text{P}^*$ 

J.E.M. Thomson, R.J.J. Stewart and M. N. Thompson

Paper V-D - Isotopic Spin Mixing in the Isobaric Analogue States of  $^{90}\text{Zr}$ 

H. J. Askin, K.J.F. Allen, R. S. Hicks, R. J. Petty and M.N. Thompson

The International Conference on Photonuclear Reactions and Applications,  
Asilomar, March 26 - 30, 1973Paper 2B4-1 The  $^9\text{Be}(\gamma, \text{Tn})$  Cross Section

R. J. Hughes, R. H. Sambell and B. M. Spicer

2B4-3 The  $^{10}\text{B}(\gamma, \text{Tn})$  and  $^{11}\text{B}(\gamma, \text{Tn})$  Cross Sections

R. J. Hughes and B. M. Spicer

2B12 De-excitation  $\gamma$ -rays following Photodisintegration of  $^{31}\text{P}$ 

L. Zalcman, J.E.M. Thomson and M. N. Thompson

2C9-3 The Photoproton Reaction on  $^{181}\text{Ta}$ A. Suzuki, K. Shoda, M. Sugawara, T. Saito, H. Miyase, S. Oikawa and J. Megaki (Tohoku University, Sendai, Japan) and M. N. Thompson  
K.J.F. Allen and H. J. Askin (University of Melbourne) and  
B. N. Sung (Seoul National University, Korea)5B4 The Photoneutron Cross Section of  $^{45}\text{Sc}$ 

R. H. Sambell and B. M. Spicer

5B12 Similarities in Photoproton Spectra from  $^{90}\text{Zr}$  and  $^{91}\text{Zr}$ 

H. J. Askin, K.J.F. Allen and M. N. Thompson (University of Melbourne), K. Shoda, M. Sugawara and H. Miyase (Tohoku University, Japan) B. N. Sung (Seoul National University, Korea)

(N.B. the extent of U.S. Army support in the work leading to papers 2C9-3 and 5B12 (above) has been the use of the PDP-15 computer in Melbourne for part of the data analysis.)

An Invited Paper at this Conference was given by Judith M. Dixon on  
"Giant Resonance Reaction Products".The Fifth Australian Institute of Nuclear Science & Engineering Conference on  
Nuclear Physics, Canberra, Australia, February 11 - 13, 1974

Paper 56 Photoprotons from Tantalum. K.J.F. Allen

57 Photonuclear Excitations of  $^{31}\text{P}$ . L. Zalcman60 Photoprotons from  $^{92}\text{Zr}$  and  $^{94}\text{Zr}$ . A. Davison and K.J.F. Allen62 Evidence for  $\alpha$ -particle clustering in nuclei. B. M. Spicer



The National Congress of the Australian Institute of Physics,  
Adelaide, South Australia, May 21 - 24, 1974

Invited paper, B. M. Spicer, Review of Experimental Nuclear Physics

The Fourth International Conference on Atomic Physics,  
Heidelberg, West Germany, July 22 - 26, 1974

Contributed paper, K-Shell Ionization by Relativistic Electrons  
Contributed Papers, pp448-9

G. R. Dangerfield and B. M. Spicer

APPENDIX 3

List of Technical Reports

- UM-P-72/14 "Graphical Presentation of Angular Distribution Coefficients"  
Judith M. Dixon
- UM-P-73/9 "Cross Sections for the Photodisintegration of  $^{32}\text{S}$  Leading to  
Excited Residual States"  
J.E.M. Thomson, M. N. Thompson and R.J.J. Stewart
- UM-P-74/22 "A Series of Lectures on Nuclear Isospin"  
K. Shoda
- UM-P-74/33 "Photoproton Analysis Computer Programs"  
K.J.F. Allen
- UM-P-75/5 "Photoprotons from  $^{92}\text{Zr}$  and  $^{94}\text{Zr}$ "  
K.J.F. Allen, A. Davison and M. N. Thompson



#### APPENDIX 4

##### List of Higher Degrees Granted

##### For the Degree of Doctor of Philosophy

E. K. Bramanis	"Correlations in Photonuclear Reactions"
G. R. Dangerfield	"Relativistic Electron K-Ionization"
R. J. Hughes	"Photonuclear Experiments - the ( $\gamma$ ,Tn) Cross Sections of $^9\text{Be}$ , $^{10}\text{B}$ and $^{11}\text{B}$ "
H. J. Askin	"Some Studies of Photoproton Emission"
R. H. Sambell	"Some Studies in Photonuclear Physics"
K.J.F. Allen	"Isospin Effects in Some Photonuclear Reactions"

##### For the Degree of Master of Science

Mrs A. McDougall	"A Particle-Hole-Rotator Coupling Model for Carbon-12"
E. D. McKenzie	"Carbon Photoneutron Cross Sections"
J. F. McKenzie	"The Automation of a Photoneutron Cross Section Experiment".